Title: Imaging of Osteoarthritis

Authors:

Ali Guermazi, MD PhD[a]

Daichi Hayashi, MD PhD[a]

Felix Eckstein, MD[b]

David J. Hunter, MBBS PhD[c]

Jeff Duryea, PhD[d]

Frank W. Roemer, MD[a]

a. Department of Radiology, Boston University School of Medicine, 820 Harrison Avenue, FGH Building 3rd Floor, Boston, MA 02118, USA

b. Institute of Anatomy and Musculoskeletal Research, Paracelsus Medical University, Strubergasse 21, 5020 Salzburg, Austria

c. Department of Rheumatology, Royal North Shore Hospital and Northern Clinical School, University of Sydney, Sydney, NSW, Australia

d. Department of Radiology, Brigham and Women's Hospital, 75 Francis Street, Boston MA 02115, USA

Corresponding author: Ali Guermazi (guermazi@bu.edu)

Email addresses: Daichi Hayashi (dhayashi@bu.edu); Felix Eckstein (felix.eckstein@pmu.ac.at) David Hunter (david.hunter@sydney.edu.au); Jeff Duryea (jduryea@bwh.harvard.edu); Frank Roemer (Frank.Roemer@klinikum-augsburg.de)

Synopsis: Osteoarthritis (OA) is the most prevalent joint disorder in the elderly, and despite on-going research, there is still no effective treatment. It has become clear in the course of research that imaging is essential for evaluating the synovial joint structures (including cartilage, meniscus, subchondral bone marrow and synovium) for diagnosis, prognosis and follow-up. Conventional radiography is still the most common, and radiographic JSW loss represents the only FDA-approved endpoint for structural disease progression in clinical trials. However, MR imaging-based studies have revealed some of the limitations of radiography. The ability of MR to image the knee as a whole organ and to directly and three-dimensionally assess cartilage morphology and composition plays a crucial role in understanding the natural history of the disease and in the search for new therapies. This article describes the roles and limitations of both conventional radiography and MR imaging while also considering the use of other modalities (e.g. ultrasound, nuclear medicine, computed tomography (CT), and CT/MR arthrography) in clinical practice and OA research. The emphasis throughout is on OA of the knee. This article is an update to the previously published article (Guermazi et al. Rheum Dis Clin N Am 2008; 34:645-687), and thus emphasizes research developments and literature evidence published since 2008, although, of course, some earlier publications are also cited.

Key Points:

1. Although conventional radiography is still the most commonly used imaging modality for clinical management of osteoarthritis patients, and loss of joint space width represents the only FDA-approved endpoint for structural disease progression in clinical trials, MR imaging-based studies have revealed some of the limitations of radiography.

2. The ability of MR to image the knee as a whole organ and to directly and three-dimensionally assess cartilage morphology and composition plays a crucial role in understanding the natural history of the disease and in the search for new therapies.

3. MR imaging of osteoarthritis can be classified into the following approaches: semiquantitative, quantitative, and compositional.

4. Ultrasound can also be useful to evaluate synovial pathology in osteoarthritis, particularly in the hand.

Keywords: osteoarthritis; imaging; radiography; MR imaging; ultrasound; CT; PET

Conventional radiography

Overview

Radiography is the simplest and least expensive imaging technique. It can detect OA-associated bony features including marginal osteophytes, subchondral sclerosis, and subchondral cysts [1]. Radiography can also determine joint space width (JSW), an indirect surrogate of cartilage thickness and meniscal integrity, but precise measurement of each of these articular structures is not possible with radiography [2]. Despite this drawback, slowing of radiographically detected joint space narrowing (JSN) is the only structural end point currently accepted by regulatory bodies in the United States (U.S. Food and Drug Administration) to prove efficacy of disease-modifying OA drugs in phase-III clinical trials. OA is radiographically defined by the presence of osteophytes [3]. Progression of JSN is the most commonly used criterion for the assessment of OA progression and the complete loss of JSW characterized by bone-on-bone contact is one of the indicators for joint replacement.

However, previously held beliefs that JSN and its changes are the only visible evidence of cartilage damage have been shown to be incorrect. Recent studies have demonstrated that alterations in the meniscus, such as meniscal extrusion or subluxation, also contribute to JSN [2]. The lack of sensitivity and specificity of radiography for the detection of articular tissue damage associated with OA, and its poor sensitivity to change at follow-up imaging, are inherent limitations of radiography.

Another limitation is the presence of variations in semiflexed knee positioning, which occur during image acquisition in trials and clinical practice despite standardization. Kinds and colleagues showed that such variations have significant influence on the quantitative measurement of various radiographic parameters of OA including JSW [4]. Thus, better

standardization needs to be achieved during radiographic acquisition. Despite these limitations, radiography remains the gold standard for structural modification in clinical trials of knee OA.

Semiquantitative assessments of knee OA features

The severity of OA can be estimated using semiquantitative scoring systems. Published atlases provide images that represent specific grades [1]. The Kellgren and Lawrence (KL) grade [5] is a widely accepted scheme used for defining the presence or absence of OA, usually using grade 2 disease as the threshold. However, KL grading has its limitations too; in particular, KL grade 3 includes all degrees of JSN, regardless of the actual extent. Felson and colleagues have suggested a modification of KL grading to improve the sensitivity to change in longitudinal knee OA studies [6]. They recommend that OA be defined by a combination of joint space loss and definite osteophytes on radiography in a knee which did not have this combination on the previous radiographic assessment. For OA progression, they recommend a focus on JSN alone using either a semiquantitative [7] or a quantitative approach.

The Osteoarthritis Research Society International (OARSI) atlas [1] takes a different tack and grades tibiofemoral JSW and osteophytes separately for each compartment of the knee. This compartmental scoring appears to be more sensitive to longitudinal radiographic changes than KL grading. A recent study using data from the OA Initiative highlighted the importance of centralized radiographic assessment in regard to observer reliability, as even expert readers apply different thresholds when scoring JSN [8].

Quantitative assessments of joint space width

Quantitative measures of JSW use a "ruler", either a physical device or a software application, to measure the JSW as the distance between the projected femoral and tibial margins

on the image (Figure 1). The femoral margin is defined as the projected edge of the bone, while the software usually determines the tibial margin as a bright band corresponding to the projection of the X-ray beam through the radio-dense cortical shell at the base of the tibial plateau. Quantification of JSW using image processing software does require a digital version of the image which can be provided for plain films by a radiographic film digitizer, or files can be analyzed directly for fully digital modalities such as computed radiography and digital radiography. Minimum JSW is the standard metric, but some groups have investigated location-specific JSW as well [9-14].

Studies using the software methods have demonstrated improved precision over the manual method and semi-quantitative scoring [15,16]. More recently, these methods have been evaluated using longitudinal knee radiographs to quantify the responsiveness to change [17]. Various degrees of responsiveness have been observed depending on the degree of OA severity, length of the follow-up, and the knee positioning protocol [10,11,13,14,18,19].

Measurements of JSW obtained from radiographs of knee OA have been found to be reliable, especially when the study lasted longer than two years and when the radiographs were obtained with the knee in a standardized flexed position [20]. Studies of hip OA have shown conflicting results when correlating JSW and symptoms. However, several studies have demonstrated that JSW can predict hip joint replacement [21].

Recent studies using radiographic evaluation of OA and associated features

A prospective observational cohort study by Harvey and colleagues associated leg length inequality of ≥1 cm with prevalent radiographic and symptomatic OA in the shorter leg, and increased odds of progressive OA in the shorter leg over 30 months [22]. This study showed that leg length inequality should be a modifiable risk factor for knee OA. Duryea and colleagues

compared the responsiveness of radiographic JSW using automated software with MR imaging-derived measures of cartilage morphometry for OA progression [19]. Results demonstrated that measures of location-specific JSW, using a software analysis of digital knee radiographic images, were comparable with MR imaging in detecting OA progression. Although the limitations of radiography are known, the study showed that when the lower cost and greater accessibility of radiography are compared to MR imaging, radiography still has a role to play in OA trials. A clinical trial by Mazzuca and colleagues showed varus malalignment of the lower limb negated the slowing of structural progression of medial JSN by doxycycline [23]. It remains to be seen if the same effect can be obtained on MR imaging-based evaluation of OA progression.

Using data from the Cohort Hip & Cohort Knee study, Kinds and colleagues showed that measuring osteophyte area (odds ratio (OR) =7.0) and minimum JSW (OR=0.7), in addition to demographic and clinical characteristics, improved the prediction of radiographic OA occurring five years later (area under curve receiver operating characteristic=0.74 vs 0.64 without radiographic features) in patients with knee pain at baseline [24]. A cross-sectional study based on the same cohort of patients showed that, in patients with early symptomatic knee OA, osteophytosis, bony enlargement, crepitus, pain, and higher BMI were associated with lower knee flexion [25]. JSN was associated with lower range of motion in all planes. In addition, osteophytosis, flattening of the femoral head, femoral buttressing, pain, morning stiffness, male gender, and higher BMI were found to be associated with poorer range of motion in the hip, in two planes.

Two publications from a large-scale Japanese population-based study demonstrated that occupational activities involving kneeling and squatting [26], as well as obesity, hypertension and dyslipidemia [27] were associated with lower medial minimum JSW when compared to

controls. Another cross sectional study found that a low level of vitamin D was associated with knee pain but not radiographic OA [28]. A longitudinal study by the same group showed accumulation of metabolic syndrome components (obesity, hypertension, dyslipidemia, and impaired glucose tolerance) is significantly related to occurrence and progression of radiographic knee OA [29].

It is interesting to note that two older methods–bone texture analysis and tomosynthesis–have experienced a revival lately. Bone texture analysis extracts information on two-dimensional trabecular bone texture from conventional radiography, that directly relates to three-dimensional bone structure [30,31]. The authors of a recent study showed that bone texture may be a predictor of progression of tibiofemoral OA. Whether bone texture correlates with other changes of subchondral bone such as MR imaging-detected bone marrow lesions (BMLs) or sclerosis remains to be seen. Tomosynthesis generates an arbitrary number of section images from a single pass of the X-ray tube. It has been shown that digital tomosynthesis improves sensitivity for depicting lesions in the chest, the breast and in rheumatoid arthritis [32-35]. However, Hayashi et al. demonstrated that tomosynthesis is more sensitive to osteophytes and subchondral cysts than radiography, using 3T MR imaging as the reference [36]. The clinical availability of these systems is currently limited, true, but the potential of this technique for OA research might be worth exploring.

MR imaging

Although not routinely used in clinical management of OA patients, MR has become a key imaging tool for OA research [37-41] thanks to its ability to visualize pathologies that are not detected on radiography, i.e. articular cartilage, menisci, ligaments, synovium, capsular structures, fluid collections and bone marrow (Figure 2-5)[42-56]. Additionally, with MR

imaging osteoarthritis can be classified into hypertrophic and atrophic phenotypes, according to the size of osteophytes [57]. Based on some of these pathological features, an MR imaging-based definition of OA has recently been proposed [58]. Tibiofemoral OA on MR imaging is defined as either (a) the presence of both definite osteophyte formation AND full thickness cartilage loss, OR (b) the presence of one of the features in (a) AND one of the following: subchondral BML or cyst not associated with meniscal or ligamentous attachments; meniscal subluxation, maceration or degenerative (horizontal) tear; partial thickness cartilage loss; and bone attrition.

With MR imaging, the four things can be achieved:

- the joint can be evaluated as a whole organ
- pathologic changes of preradiographic OA can be detected at a much earlier stage of the disease
- physiologic changes within joint tissues (e.g. cartilage and menisci) can be assessed before morphologic changes become apparent
- multiple tissue changes can be monitored simultaneously over several time points (Figure 6)

Importantly, the use of MR imaging has led to significant findings about the association of pain with BMLs [59] and synovitis [60], with implications for future OA clinical trials. Systematic reviews have demonstrated that MR imaging biomarkers in OA have concurrent and predictive validity, with good responsiveness and reliability [61,62]. The Osteoarthritis Research Society International (OARSI) - US Food and Drug Administration working group now recommends MR imaging as a suitable imaging tool for cartilage morphology in clinical trials[37].

The following sections focus on recent advances in the use of MR as an imaging tool in OA research. First, MR imaging-based semiquantitative OA scoring systems that were published after 2008 are reviewed. Second, research efforts in quantitative MR imaging techniques are described. Last, developments in compositional/physiologic MR imaging techniques are reviewed.

Semiquantitative MR imaging scoring systems for knee OA

In addition to the three well-established scoring systems–the Whole Organ Magnetic Resonance Imaging Score (WORMS) [63], the Knee Osteoarthritis Scoring System (KOSS) [64], and the Boston Leeds Osteoarthritis Knee Score (BLOKS) [65]–a new scoring system called the MR Imaging Osteoarthritis Knee Score (MOAKS) has been added to the literature (Table 1, 2). Of the three systems, WORMS and BLOKS have been widely disseminated and used, though only a limited number of studies have directly compared the two systems. Two recent studies by Lynch et al and Felson et al were helpful in identifying the relative strengths and weaknesses of the two systems in regard to certain features assumed to be most relevant to the natural history of the disease, including cartilage, meniscus and BMLs [66,67]. WORMS and BLOKS have their weaknesses and it may be difficult for investigators to choose which is more suitable for the particular aims of the study they are planning. For instance, the WORMS meniscal scoring method mixes multiple constructs, while in BLOKS, application of the BML scoring system is cumbersome and complex, and some of the scoring appears redundant. Additionally, both these systems have undergone unpublished modifications that make it difficult for general readers to determine the differences between the original description and how they have been applied in later research. The use of within-grade changes for longitudinal assessment of cartilage damage and BMLs is a good example [68]. Within-grade scoring describes progression or improvement

of a lesion that does not meet the criteria of a full grade change but does represent a definite visual change. In the original publication of WORMS, for example, there was no mention of scoring of within-grade changes as the WORMS publication only used a cross-sectional dataset. It has become common practice to incorporate these within-grade changes whenever longitudinal cartilage assessment is contemplated. A recent study by Roemer and colleagues demonstrated that within-grade changes in semiquantitative MR imaging assessment of cartilage and BMLs are valid and their use may increase the sensitivity of semiquantitative readings in detecting longitudinal changes in these structures [68].

Alas, there has never been a published correction or an addendum to the original WORMS publication. The effort to evolve semiquantitative scoring methods that circumvent the limitations of WORMS and BLOKS led to the development of MOAKS. By integrating expert readers' experience with all of the available scoring tools and the published data comparing different scoring systems, MOAKS refined the scoring of BMLs, added subregional assessment, omitted some redundancy in cartilage and BML scoring, and refined elements of meniscal morphology.

For BML size assessment, the threshold for grading in terms of percentage of subregional volume was modified. Also, rather than a lesion-based approach, the subregion-based approach of WORMS was incorporated. The number of lesions is counted, but the percentage of BML in the area of the adjacent subchondral plate is no longer recorded. There is only one cartilage score using a WORMS-like subregional approach. Synovitis as detected in the form of high signal intensity in the Hoffa fat pad is now called ”Hoffa-synovitis”. Effusion was renamed ”effusion-synovitis”, as high signal within the joint cavity on T2-weighted images incorporates both joint fluid (i.e. effusion) and synovial thickening (i.e. synovitis). A detailed differentiation of the

different types of meniscal tears, meniscal hypertrophy, partial maceration and progressive partial maceration has been incorporated allowing for detailed assessment of meniscal damage over time (Figure 7). The scoring of non-cystic BML percentage, osteophytes, meniscal extrusion and signal, ligaments and periarticular features remain unchanged from BLOKS.

The MOAKS system is currently being deployed in the Meniscal Tear in Osteoarthritis Research (MeTeOR) trial [69] and the Pivotal Osteoarthritis Initiative Magnetic Resonance Imaging Analyses (POMA) [70]. However, it is a new scoring system and needs more data to demonstrate its validity and reliability when applied to OA studies.

Synovitis is an important feature of OA, with a demonstrated association with pain [60,71]. Although synovitis can be evaluated with non-contrast-enhanced MR imaging by using the presence of signal changes in Hoffa fat pad or joint effusion as an indirect marker of synovitis, only contrast-enhanced MR imaging can reveal the true extent of synovial inflammation (Figure 4) [72]. Table 3 summarizes currently available comprehensive scoring systems for synovitis in knee OA based on contrast-enhanced MR imaging. These scoring systems could potentially be used in clinical trials of new OA drugs that target synovitis.

Semiquantitative MR imaging whole organ scoring system for hand OA

Conventional radiography is still the imaging modality of choice clinically for OA of the hand, but the use of more sensitive imaging techniques such as ultrasound and MR imaging is becoming more common, especially for research purposes. However, the literature concerning MR imaging of pathological features of hand OA is still sparse, and studies have been performed without applying standardized methods [73-79]. In 2011, Haugen et al proposed a semiquantitative MR imaging scoring system for hand OA features, called the Oslo Hand OA MRI Score (OHOA-MRI) [80]: it incorporates osteophyte presence and joint space narrowing (0-

3 scale) and malalignment (absence/presence) in analogue to the OARSI atlas [1]. Cysts and collateral ligament pathology are also recorded as absent or present. These features are assessed at eight locations (distal and proximal interphalangeal (DIP and PIP) joints of the second, third, fourth and fifth fingers) of the dominant hand using an extremity 1.0 T MR system. An atlas is included in the publication to facilitate scoring. Each MR image feature was analyzed and stratified for joint groups and as aggregated scores (i.e. DIP and PIP). Key features such as synovitis, flexor tenosynovitis, erosions, osteophytes, joint space narrowing and BMLs showed good to very good intra- and inter-reader reliability [81].

Using this scoring system, Haugen et al showed that MR imaging could detect approximately twice as many joints with erosions and osteophytes as conventional radiography ($p<0.001$), but identification of joint space narrowing, cysts and malalignment was similar [82]. The prevalence of most MR imaging features increased with radiographic severity, but synovitis was more frequent in joints with mild osteoarthritis than with moderate/severe osteoarthritis. The same group of investigators also showed in another study that MR imaging-assessed moderate/severe synovitis, BMLs, erosions, attrition and osteophytes were associated with joint tenderness independently of each other [83]. Weaker associations were found between the sum score of MR imaging-defined attrition and the Functional Index of Hand Osteoarthritis (FIHOA), and between the sum score of osteophytes and grip strength [83]. These studies demonstrated that some of the semiquantitatively assessed MR imaging features of hand OA may be potential targets for therapeutic interventions.

Semiquantitative MR imaging whole organ scoring system for hip OA

Compared to knee OA, few studies have focused on the hip joint, and only one used an approach similar to the ”whole-organ” evaluation of knee OA [84,85]. The hip joint has a spherical

structure and its very thin covering of articular hyaline cartilage makes MR imaging assessment of the hip much more challenging than the knee [86]. Patients with OA of the hip often have to be followed for a long time to assess the natural course of joint pathology, or to evaluate surgical or pharmacological treatment effects. Non-invasive, follow-up methods are necessary, and surrogate markers based on MR imaging would be very useful. Following this line of thought, a novel tool for use in observational studies and clinical trials of hip joints, a whole-organ semiquantitative multi-feature scoring method called the Hip Osteoarthritis MRI Scoring System (HOAMS) was introduced by Roemer et al in 2011 [87].

In HOAMS, fourteen articular features are assessed: cartilage morphology, subchondral bone marrow lesions, subchondral cysts, osteophytes, acetabular labrum, synovitis (only scored when contrast-enhanced sequences were available), joint effusion, loose bodies, attrition, dysplasia, trochanteric bursitis/insertional tendonitis of the greater trochanter, labral hypertrophy, paralabral cysts and herniation pits at the supero-lateral femoral neck. Cartilage and osteophytes are scored on a 0-4 scale; BMLs, subchondral cysts and labral pathology are graded 0-3; synovitis and effusion are graded 0-2; and all other lesions are scored 0 (absent) or 1 (present). Cartilage morphology is scored in nine subregions, and BMLs and subchondral cysts in 15 subregions for acetabular and femoral subchondral bone marrow assessment. MR imaging sequences acquired in the protocol include coronal and axial non fat-suppressed T1-weighted spin echo, coronal and sagittal proton density-weighted fat-suppressed fast spin-echo, and where indicated coronal and axial contrast-enhanced T1-weighted sequences.

Whether this scoring tool is similarly applicable to longitudinal studies, particularly with regard to its responsiveness and predictive validity remains to be seen. HOAMS demonstrated satisfactory reliability and good agreement concerning intra- and inter-observer assessment, but

further validation, assessment of responsiveness and iterative refinement of the scoring system are still needed to maximize its utility in clinical trials and epidemiological studies.

Quantitative cartilage morphometry

Quantitative measurement of cartilage morphology segments the cartilage image (Figure 8,9) and exploits the three-dimensional nature of MR imaging data sets to evaluate tissue dimensions (such as thickness and volume) or signal as continuous variables. Examples of nomenclature for MR imaging-based cartilage measures were proposed by Eckstein and colleagues [88]:. VC = cartilage volume; tAB = total area of subchondral bone; dAB = denuded area of subchondral bone, ThCtAB.Me = mean cartilage thickness over the tAB. As many of these measures are strongly related, Buck and colleagues identified an efficient subset of core measures–tAB, and dAB–that can provide a comprehensive description of cartilage morphology and its longitudinal changes, in knees with or without OA [89]. The same group also proposed a strategy (the ordered values approach) for more efficiently analyzing longitudinal changes in (subregional) cartilage thickness [90] and found that determining the magnitude of subregional cartilage thickness changes independent of anatomic location provided improved discrimination between OA participants and healthy subjects longitudinally. Further, the ordered values approach was found to be superior in detecting risk factors of OA progression [91]. Wirth and colleagues proposed an "extended ordered values approach" with better discrimination of cartilage thickness changes in KL grade 2 vs. KL grade3 knees than measures of total plate and subregional cartilage thickness or changes in radiographic JSW [92].

Quantitative measurements of cartilage volume and thickness have been used in several intervention studies. Ding and colleagues examined the associations between non-steroidal anti-inflammatory drugs (NSAIDs) and changes in knee cartilage volume [93]. Comparing users of

cyclooxygenase-2 inhibitors with NSAIDs users, the latter had more knee cartilage volume loss. Raynauld and colleagues after evaluating the effect of celecoxib on cartilage volume loss over one year in knee OA [94], found that the drug did not show a protective effect on knee cartilage loss. Wei and colleagues conducted a cross-sectional study of middle-aged and elderly women and showed parity, but not use of hormone replacement therapy or oral contraceptives, was independently associated with lower cartilage volume primarily in the tibial compartment [95]. Joint distraction was found to be very effective in regenerating cartilage, by increasing its thickness and decreasing denuded areas of subchondral bone, and with the effects lasting for months after the intervention [96]

Bennell and colleagues showed that increased dynamic medial knee load was associated with a greater loss of medial cartilage volume over one year [97]. Eckstein and colleagues compared knees with frequent pain with knees without pain, and found higher rates of (medial femorotibial) cartilage loss over one year in the painful knees compared to the painless knees [98]. Adjustment or stratification for radiographic disease stage did not affect this association. The authors concluded that enrolling participants with frequent knee pain in clinical trials could increase the observed rate of structural progression. The same group also showed that: radiographic and MR cartilage morphometry features suggestive of advanced OA (high KL grade) appear to be associated with greater cartilage thickness loss [99, 100]. Knees with early radiographic OA (KL grade 2) display thicker cartilage than healthy reference knees or the contralateral knees without radiographic findings of OA, specifically in the external femoral subregions [101, 102].

Quantitative measures of articular cartilage structure, such as cartilage thickness loss and denuded areas of subchondral bone have been shown to predict an important clinical outcome, i.e.

knee replacement [103]. However, long-term observations are needed to achieve robust results on tibiofemoral cartilage thickness loss in individual knees in observational OA studies, by comparing one year with two and four year rates of change in OA knees [104]. Further, investigators intending to use the quantitative morphometry approach in a multicenter study should be aware of at least one pitfall: quantitative data collected from different segmentation teams cannot be pooled unless equivalence is demonstrated for the cartilage metrics of interest: Schneider and colleagues showed that segmentation-team differences dominated measurement variability in most cartilage regions for all image series [105].

Functional studies in healthy subjects reported nocturnal changes of cartilage thickness, with more morning post-exercise deformation than evening post-exercise deformation [106]. Osteoarthritic cartilage tended to show more deformation upon loading than healthy cartilage, suggesting that knee OA affects the mechanical properties of cartilage, and the pattern of in vivo deformation indicated that cartilage loss in OA progression is mechanically driven [107]. Similarly, a correlation between changes in cartilage thickness and those in a molecular serum marker (i.e. cartilage oligomeric matrix protein (COMP)) after drop landing was reported [108].

Quantitative MR imaging analysis of tissues other than cartilage

Several authors have reported studies using MR imaging to quantitatively evaluate the menisci. Wirth and colleagues presented a technique for three-dimensional and quantitative analysis of meniscal shape, position and signal intensity [109], which was shown to display adequate inter-observer and intra-observer precision [110,111]. When examining healthy reference subjects using these techniques, the authors reported that meniscus surface area strongly corresponds with (ipsilateral) tibial plateau area across both sexes, and that tibial coverage by the meniscus is similar between men and women.

Swanson et al developed an algorithm to semi-automatically segment the meniscus in a series of MR images [112]. Their method produced accurate and consistent segmentations of the meniscus when compared to the manual segmentations. Wenger and colleagues described an association between knee pain and meniscal extrusion using a between-knee, intra-person comparison using three-dimensional measures of extrusion [113].

Other than menisci, investigators have used quantitative MR imaging to assess BMLs [114,115], synovitis [116] and joint effusion [117]. However, it should be kept in mind that using segmentation approaches for ill-defined lesions such as BMLs is more challenging than segmentation of clearly delineated structures such as cartilage, menisci and effusion [41].

Compositional MR imaging of cartilage and menisci

Compositional MR imaging can assess the biochemical properties of different joint tissues and thus is very sensitive to early, pre-morphologic changes that cannot be seen on conventional MR imaging. The vast majority of studies applying compositional MR imaging have focused on cartilage, although the technique can also be used to assess other tissues such as the meniscus or ligaments. Compositional imaging of cartilage matrix changes can be performed using advanced MR imaging techniques such as dGEMRIC (Figure 10), T1 rho, and T2 mapping (Figure 11). For detailed descriptions of these techniques, readers are referred to the published review articles [118,119].

In a placebo-controlled double-blind pilot trial of collagen hydrolysate for mild knee OA, McAlindon and colleagues [120] demonstrated that the dGEMRIC score increased in tibial cartilage regions of interest in subjects receiving collagen hydrolysate, and decreased in the placebo group. A significant difference was observed at 24 weeks. It will be of interest to see if macroscopic cartilage changes are associated with those dGEMRIC findings in future studies.

Another study [121] showed an increase in dGEMRIC indices of knee cartilage in asymptomatic untrained women who were enrolled in a 10-week running program, when compared to sedentary controls. Souza and colleagues [122] showed that acute loading of the knee joint resulted in a significant decrease in T1 rho and T2 relaxation times of the medial tibiofemoral compartment, and especially in cartilage regions with small focal defects. These data suggest that changes of T1 rho values under mechanical loading may be related to the biomechanical and structural properties of cartilage.

Hovis and colleagues reported that light exercise was associated with low cartilage T2 values but moderate and strenuous exercise was associated with high T2 values in women, suggesting that activity levels can effect cartilage composition [123]. Another study looked at the normal control group at baseline and two years later and found a high prevalence of structural abnormalities and a significant increase in cartilage T2 values in the tibiofemoral but not the patellofemoral joint [124]. In an interventional study assessing the effect of weight loss on articular cartilage, Anandacoomarasamy and colleagues reported that improved articular cartilage quality was reflected as an increase in the dGEMRIC index over one year for the medial but not the lateral compartment [125]. This finding highlights the role of weight loss in possible clinical and structural improvement.

Williams and colleagues described intrameniscal biochemical alterations using ultra-short echo time-enhanced T2* mapping [126]. The authors found significant elevations of ultra-short echo time-enhanced-T2* values in the menisci of subjects with ACL injuries but who showed no clinical evidence of subsurface meniscal abnormality.

Novel compositional techniques have been explored further. Raya and coworkers found that in vivo diffusion tensor imaging with a 7T MR system could distinguish OA knees from

non-OA knees better than T2 mapping [127]. Other work on 7T systems reported on the reproducibility of the method in vivo [128,129]. Another compositional technique that might reward further exploration is T2* mapping of cartilage [130].These techniques show promise, but they will need to be practical and deployable using standard MR imaging systems before they can be widely used as a research or a clinical diagnostic tool.

Ultrasound

Ultrasound imaging allows multiplanar and real time imaging without radiation exposure at relatively low cost. It can offer reliable assessment of OA-associated features, including inflammatory and structural abnormalities, without contrast administration [131]. Limitations of ultrasound include that it is an operator-dependent technique and that the physical properties of sound limit its ability to assess deeper articular structures and the subchondral bone (Figure 12).

Ultrasound is useful for evaluation of cortical erosive changes and synovitis in inflammatory arthritis [132]. In OA, the ability to detect synovial pathology is the major advantage ultrasound has over conventional radiography. Current generation ultrasound technology can detect synovial pathologies including hypertrophy, increased vascularity and the presence of synovial fluid in joints affected by arthritis (Figure 13) [131]. The Outcome Measures in Rheumatoid Arthritis Clinical Trials (OMERACT) Ultrasonography Taskforce reported an ultrasound-definition of synovial hypertrophy as “abnormal hypoechoic (relative to subdermal fat, but sometimes may be isoechoic or hyperechoic) intra-articular tissue that is non-displaceable and poorly compressible and which may exhibit Doppler” [133]. Although this definition was developed for use in rheumatoid arthritis, it may also be applied to OA because the difference in synovial inflammation between OA and rheumatoid arthritis is largely quantitative rather than qualitative [131].

A preliminary ultrasonographic scoring system for features of hand OA was published recently [134]. This scoring system included evaluation of grey-scale synovitis and power Doppler signal in 15 joints of the hand. These features were assessed for their presence/absence and if present were scored semiquantitatively using a 1-3 scale. Overall, the reliability exercise demonstrated moderately good intra- and inter-reader reliability. This study has demonstrated that an ultrasound outcome measure suitable for multicenter trials assessing hand OA is feasible and likely to be reliable, and has provided a foundation for further development.

Ultrasound has been increasingly used for assessment of OA of the hand (Figure 13). Kortekaas and colleagues showed that ultrasound-detected osteophytes and JSN are associated with hand pain [135]. In a more recent study, the same group of authors showed that signs of inflammation appear more frequently on ultrasound in erosive OA hands than in non-erosive OA hands, not only in erosive joints but also in non-erosive joints [136]. This finding suggests the presence of an underlying systemic cause for erosive evolution. Klauser and colleagues evaluated the efficacy of weekly ultrasound-guided intra-articular injections of hyaluronic acid [137]. A decrease in pain correlated with a decrease in synovial thickening and power Doppler ultrasound score between baseline and the end of therapy. To take advantage of ultrasound and MR imaging, Iagnocco and colleagues performed integrated MR imaging and ultrasound real-time fusion imaging in hand and wrist OA, and found a high concordance of the bony profile visualization at the level of osteophytes [77].

Evaluation of synovitis in OA of the knee has also been documented (Figure 14) [102]. A cross sectional, multi-center European study supported by EULAR analyzed 600 patients with painful knee OA, and found that ultrasound-detected synovitis correlated with advanced radiographic OA and clinical signs and symptoms suggestive of an inflammatory “flare.”

However, ultrasound-detected synovitis was not a predictor of subsequent joint replacement. Additionally, ultrasound signs of synovitis were found to be reflected metabolically by markers of joint tissue metabolism [139]. Saarakkala and colleagues evaluated the diagnostic performance of knee ultrasound for the detection of degenerative changes of articular cartilage, using arthroscopic findings as the reference [140]. They found that positive ultrasound findings are strong indicators of cartilage degeneration, but negative findings do not exclude cartilage degeneration. Kawaguchi and colleagues used ultrasound to look at medial radial displacement of the meniscus in the supine weight-bearing positions [141]. They showed the medial meniscus was significantly displaced radially by weight-bearing in control knees and in those with KL grade 1-3. Significant differences were noted between KL grade ≥2 knees and controls in the supine and the standing positions, and displacement increased in all weight-bearing knees at one year follow-up, except for KL grade 4 knees.

Chao and colleagues assessed whether inflammation on ultrasound can predict clinical response to intra-articular corticosteroid injections in patients with knee OA [142]. Somewhat unexpectedly, there was a significantly greater improvement in pain among non-inflammatory patients than among inflammatory patients 12 weeks post injection. A small sample size, a lack of power Doppler imaging, and the fact that only the suprapatellar pouch was imaged, could have led to these unexpected results. Wu and colleagues investigated the association of ultrasound features with pain and the functional scores in patients with equal radiographic grades of knee OA in both knees [143]. They showed ultrasound-detected inflammatory features, including suprapatellar effusion and medial compartment synovitis, were positively and linearly associated with knee pain in motion. Medial compartment synovitis was also degree-dependently associated with pain at rest and with the presence of medial knee pain. These findings confirmed

the association between synovitis and knee pain, which has also been reported in MR imaging-based studies [60].

Nuclear medicine

Use of 99mTc-hydroxymethane diphosphonate (HDP) scintigraphy and 2-^{18}F-fluoro-2-deoxy–D-glucose (18-FDG) or 18F-fluoride (18-F^-) positron emission tomography (PET) for assessing OA have been described in the literature (Figure 15,16) [144]. Bone scintigraphy is a simple examination that can provide a full-body survey that helps to discriminate between soft tissues and bone origin of pain, and to locate the site of pain in patients with complex symptoms [144]. 18-FDG PET can demonstrate the site of synovitis and bone marrow lesions associated with OA [145]. 18-F^- PET can be used for bone imaging; the amount of tracer uptake depends on the regional blood flow and bone remodeling conditions. An animal study by Umemoto and colleagues using a rat OA model showed that uptake of 18-F^- was significantly higher in knees that had undergone anterior cruciate ligament transection than in sham-operated knees, and was higher in all the compartments of the tibiofemoral joint eight weeks postoperatively [146]. An in vivo study by Temmerman and colleagues demonstrated a significant increase in bone metabolism in the proximal femur of patients with symptomatic hip OA [147]. These studies showed that 18-F^- PET is a potentially useful technique for early detection of OA changes.

Another imaging technique in the nuclear medicine category is single photon emission tomography (SPECT). Currently, researchers are searching for a cartilage-specific radiopharmaceutical agent that can be applied to OA imaging. A recent ex vivo study by Cachin and colleagues using 99mTc-N-triethylammonium-3-proyl-[15]ane-N5 (NTP 15-5), which binds to cartilage, quantified the uptake by human articular cartilage relative to bone 99m-Tc-HDP radiotracer [148]. Visual analysis of fused SPECT-CT slices showed selective, intense 99mTc-

NTP 15-5 accumulation in articular cartilage, whereas 99mTc-HDP binding was low. A cartilage defect visualized on CT was associated with focal decreased uptake of 99m-Tc-NTP 15-5. Thus, it is hoped this agent may be applied to human cartilage molecular imaging and clinical applications in OA staging and monitoring.

Limitations of radioisotope methods include poor anatomical resolution and the use of ionizing radiation. However, there are ways to overcome these issues. Hybrid technologies such as PET-CT and PET-MR imaging combine functional imaging with high resolution anatomical imaging. A study by Moon and colleagues showed PET-CT could detect active inflammation in patients with OA of the shoulder [149]. Techniques to achieve the optimum registration of PET and MR images are being developed [150]. Moreover, PET scanners that image small parts of the body have been developed [151]. Although originally developed for breast imaging, these small-part scanners may be useful for imaging of joints [144]. The small-part PET scanners have the advantages of lower operating costs and lower radiation exposure, while retaining high spatial resolution and sensitivity for detection of lesions.

CT

CT is more useful than MR imaging for depicting cortical bone and soft tissue calcifications. It has an established role in assessing facet joint OA of the spine in both clinical and research settings [152]. Using a CT-based semiquantitative grading system of facet joint OA, a population-based study by Kalichman and colleagues showed a high prevalence of facet joint OA and that the prevalence of facet joint OA increases with age, with the highest prevalence at the L4-L5 spinal level [153]. Also, in the same cohort of subjects, several associations were observed: self-reported back pain with spinal stenosis [154]; abdominal aortic calcification with facet joint OA [155]; obesity with higher prevalence of facet joint OA [156]; and increasing age

with higher prevalence of disc narrowing, facet joint OA, and degenerative spondylolisthesis [156]. A recent animal study by Kim and colleagues used micro-CT to assess the cartilage alterations in the facet joint of rats, and showed that monodoium iodoacetate injection into facet joints provided a useful model for the study of OA changes in the facet joint and indicated that facet joint degeneration is a major cause of low back pain [157].

CT and MR arthrography

Arthrography using CT or MR imaging enables evaluation of damage to articular cartilage with a high anatomical resolution in multiple planes. CT arthrography can be performed using a single (iodine alone) or double-contrast (iodine and air) technique [144]. In general, the single-contrast technique is considered easier to perform and to cause less pain to patients [158]. To avoid beam-hardening artifacts, the contrast material can be diluted with saline or local anesthetics [144]. For MR arthrography, gadolinium-DTPA is injected intra-articularly to delineate superficial cartilage defects. The optimum concentration of gadolinium-DTPA varies depending on the magnetic field strength of the MR system [159]. It has been shown that iodine-based and gadolinium-based contrast agents can be mixed, enabling combined MR arthrography and CT arthrography examinations [160]. These arthrographic examinations have a low risk of infection from the intra-articular injection [161]. Other risks include pain and vasovagal reactions, and systemic allergic reactions. CT arthrography exposes patients to radiation but MR arthrography does not.

At present, CT arthrography is the most accurate method for evaluating cartilage thickness. It offers high spatial resolution and high contrast between the low attenuating cartilage and high attenuating superficial (contrast material filling the joint space) and deep (subchondral bone) boundaries [144]. Cadaveric studies have shown that CT arthrography is more accurate

than MR imaging [162] or MR arthrography [163]. However, a more recent study showed evaluation of hip cartilage thickness in the coronal plane by MR arthrography is similarly accurate compared to CT arthrography (Figure. 17) [164]. For other planes, CT arthrography showed better diagnostic performance than MR arthrography.

Superficial focal cartilage lesions are well delineated by both arthrographic techniques and appear as areas filled with the intra-articular contrast agent. Again, CT arthrography offers higher spatial resolution as well as higher contrast between the cartilage and the intra-articular contrast agent filling the joint space, leading to a high degree of confidence in depicting these lesions with a higher inter-reader reproducibility [165].

Regarding subchondral changes, MR arthrography is the only technique that allows delineation of subchondral bone marrow lesions on the fluid-sensitive sequences with fat suppression [144]. CT arthrography is better than MR arthrography at depicting subchondral bone sclerosis and osteophytes. Both techniques enable visualization of central osteophytes, which are associated with more severe changes of OA than marginal osteophytes [166].

Because of the high cost (due to the use of contrast agents), invasive nature and potential, albeit low, risk associated with intra-articular injection, arthrographic examinations are rarely used in large scale clinical or epidemiological OA studies. However, arthrography has been used in a small-scale clinical study of post-traumatic OA [167]. Tamura and colleagues used high-resolution CT arthrography to examine the 3D progression pattern of early acetabular cartilage damage in 32 patients with hip dysplasia [168]. They found the lateral-medial ratio, which was defined as cartilage thickness in the lateral zone divided by that in the medial zone, may be a sensitive index for quantifying early cartilage damage associated with extent of labral disorders.

Summary

Since publication of the previous edition of this review article in 2008, the OA imaging field has been greatly driven by publically available images and analyses that have come out of the Osteoarthritis Initiative (OAI). OAI study design, image archive, and available image analyses and science have been recently summarized in a perspective [38]. In a research setting, conventional radiography is still commonly used to semiquantitatively and quantitatively evaluate structural OA features, such as osteophytes and JSN. Radiographic JSW measurement is still a recommended option for trials of structural modification, with the understanding that the concept of JSW represents a number of pathologies including cartilage and meniscal damage, and trial duration may be long. MR imaging is the currently most important imaging modality for research into OA, and investigators may select from semiquantitative, quantitative and compositional techniques, depending on the aims of the study. Ultrasound is commonly used in hand OA studies and is particularly useful for evaluation of synovitis. Nuclear medicine, CT and CT-MR arthrography can also be used for evaluation of OA features, but they are rarely used in large-scale clinical or epidemiological studies.

Disclosure statement:

This article has been written as an update to the previously published review article in 2008. As such, there are some contents that overlap and/or reused from that article. We would like to thank those who are not listed as an author in this article, but were co-authors of the previous edition (Deborah Burstein, Philip Conaghan, Marie-Pierre Hellio Le Graverand-Gastineau, and Helen Keen).

Role of the funding source

No funding received.

Competing interests

Dr. Guermazi has received consultancies, speaking fees, and/or honoraria from Genzyme, Stryker, Merck Serono, Novartis and Astra Zeneca and is the President of Boston Imaging Core Lab (BICL), a company providing image assessment services. He received a research grant from General Electric Healthcare. Dr. Roemer is Chief Medical Officer and shareholder of BICL. Dr. Roemer has received consultancies, speaking fees, and/or honoraria from Merck Serono and the National Institutes of Health. Dr. Eckstein has received consultancies, speaking fees, and/or honoraria from Merck Serono, Sanofi, Novartis, Abbot, Medtronic, Bioclinica and Synthes and is CEO and shareholder of Chondrometrics GmbH, a company providing image analysis services.

References

1. Altman RD, Gold GE. Atlas of individual radiographic features in osteoarthritis, revised. Osteoarthritis Cartilage 2007;15 Suppl A:A1-56.

2.Hunter DJ, Zhang YQ, Tu X, et al. Change in joint space width: hyaline articular cartilage loss or alteration in meniscus? Arthritis Rheum 2006;54:2488-95.

3.Altman R, Asch E, Bloch D, et al. Development of criteria for the classification and reporting of osteoarthritis. Classification of osteoarthritis of the knee. Diagnostic and Therapeutic Criteria Committee of the American Rheumatism Association. Arthritis Rheum 1986;29:1039-49.

4.Kinds MB, Vincken KL, Hoppinga TN, et al. Influence of variation in semiflexed knee positioning during image acquisition on separate quantitative radiographic parameters of osteoarthritis, measured by Knee Images Digital Analysis. Osteoarthritis Cartilage 2012;20:997-1003.

5.Kellgren JH, Lawrence JS. Radiological assessment of osteo-arthrosis. Ann Rheum Dis 1957;16:494-502.

6.Felson DT, Niu J, Guermazi A, Sack B, Aliabadi P. Defining radiographic incidence and progression of knee osteoarthritis: suggested modifications of the Kellgren and Lawrence scale. Ann Rheum Dis 2011;70:1884-6.

7.Felson DT, Nevitt MC, Yang M, et al. A new approach yields high rates of radiographic progression in knee osteoarthritis. J Rheumatol 2008;35:2047-54.

8.Guermazi A, Hunter DJ, Li L, et al. Different thresholds for detecting osteophytes and joint space narrowing exist between the site investigators and the centralized reader in a multicenter knee osteoarthritis study--data from the Osteoarthritis Initiative. Skeletal Radiol 2012;41:179-86.

9. Duryea J, Zaim S, Genant HK. New radiographic-based surrogate outcome measures for osteoarthritis of the knee. Osteoarthritis Cartilage 2003;11:102-10.

10. Chu E, DiCarlo JC, Peterfy C, et al. Fixed-location joint space width measurement increases sensitivity to change in osteoarthritis. Osteoarthritis Cartilage 2007;15:S192.

11. Neumann G, Hunter D, Nevitt M, et al. Location specific radiographic joint space width for osteoarthritis progression. Osteoarthritis Cartilage. 2009;17:761-5.

12. Beattie KA, Duryea J, Pui M, et al. Minimum joint space width and tibial cartilage morphology in the knees of healthy individuals: a cross-sectional study. BMC Musculoskelet Disord. 2008;9:119.

13. Duryea J, Hunter DJ, Nevitt MC, et al. Study of location specific lateral compartment radiographic joint space width for knee osteoarthritis progression: analysis of longitudinal data from the Osteoarthritis Initiative (OAI). Osteoarthritis Cartilage 2008;16:S168.

14. Nevitt MC, Peterfy C, Guermazi A, et al. Longitudinal performance evaluation and validation of fixed-flexion radiography of the knee for detection of joint space loss. Arthritis Rheum. 2007;56:1512-20.

15.Duryea J, Li J, Peterfy CG, Gordon C, Genant HK. Trainable rule-based algorithm for the measurement of joint space width in digital radiographic images of the knee. Medical physics 2000;27:580-91.

16.Marijnissen AC, Vincken KL, Vos PA, et al. Knee Images Digital Analysis (KIDA): a novel method to quantify individual radiographic features of knee osteoarthritis in detail. Osteoarthritis Cartilage 2008;16:234-43.

17.Neumann G, Hunter D, Nevitt M, et al. Location specific radiographic joint space width for osteoarthritis progression. Osteoarthritis Cartilage 2009;17:761-5.

18. Benichou OD, Hunter DJ, Nelson DR, et al. One-year change in radiographic joint space width in patients with unilateral joint space narrowing: data from the Osteoarthritis Initiative. Arthritis Care Res (Hoboken). 2010;62:924-31.

19.Duryea J, Neumann G, Niu J, et al. Comparison of radiographic joint space width with magnetic resonance imaging cartilage morphometry: analysis of longitudinal data from the Osteoarthritis Initiative. Arthritis Care Res (Hoboken) 2010;62:932-7.

20.Reichmann WM, Maillefert JF, Hunter DJ, Katz JN, Conaghan PG, Losina E. Responsiveness to change and reliability of measurement of radiographic joint space width in osteoarthritis of the knee: a systematic review. Osteoarthritis Cartilage 2011;19:550-6.

21.Chu Miow Lin D, Reichmann WM, Gossec L, Losina E, Conaghan PG, Maillefert JF. Validity and responsiveness of radiographic joint space width metric measurement in hip osteoarthritis: a systematic review. Osteoarthritis Cartilage 2011;19:543-9.

22.Harvey WF, Yang M, Cooke TD, et al. Association of leg-length inequality with knee osteoarthritis: a cohort study. Ann Intern Med 2010;152:287-95.

23.Mazzuca SA, Brandt KD, Chakr R, Lane KA. Varus malalignment negates the structure-modifying benefits of doxycycline in obese women with knee osteoarthritis. Osteoarthritis Cartilage 2010;18:1008-11.

24. Kinds MB, Marijnissen AC, Vincken KL, et al. Evaluation of separate quantitative radiographic features adds to the prediction of incident radiographic osteoarthritis in individuals with recent onset of knee pain: 5-year follow-up in the CHECK cohort. Osteoarthritis Cartilage. 2012;20:548-56.

25. Holla JF, Steultjens MP, van der Leeden M, et al. Determinants of range of joint motion in patients with early symptomatic osteoarthritis of the hip and/or knee: an exploratory study in the CHECK cohort. Osteoarthritis Cartilage. 2011;19:411-9.

26.Muraki S, Oka H, Akune T, et al. Association of occupational activity with joint space narrowing and osteophytosis in the medial compartment of the knee: the ROAD study (OAC5914R2). Osteoarthritis Cartilage 2011;19:840-6.

27.Yoshimura N, Muraki S, Oka H, Kawaguchi H, Nakamura K, Akune T. Association of knee osteoarthritis with the accumulation of metabolic risk factors such as overweight, hypertension, dyslipidemia, and impaired glucose tolerance in Japanese men and women: the ROAD study. J Rheumatol 2011;38:921-30.

28.Muraki S, Dennison E, Jameson K, et al. Association of vitamin D status with knee pain and radiographic knee osteoarthritis. Osteoarthritis Cartilage 2011.;19:1301-6.

29.Yoshimura N, Muraki S, Oka H, et al. Accumulation of metabolic risk factors such as overweight, hypertension, dyslipidaemia, and impaired glucose tolerance raises the risk of occurrence and progression of knee osteoarthritis: a 3-year follow-up of the ROAD study. Osteoarthritis Cartilage 2012;20:1217-26.

30.Pothuaud L, Benhamou CL, Porion P, Lespessailles E, Harba R, Levitz P. Fractal dimension of trabecular bone projection texture is related to three-dimensional microarchitecture. J Bone Miner Res 2000;15:691-9.

31.Apostol L, Boudousq V, Basset O, et al. Relevance of 2D radiographic texture analysis for the assessment of 3D bone micro-architecture. Medical physics 2006;33:3546-56.

32.Dobbins JT, 3rd, McAdams HP. Chest tomosynthesis: technical principles and clinical update. Eur J Radiol 2009;72:244-51.

33.Stevens GM, Birdwell RL, Beaulieu CF, Ikeda DM, Pelc NJ. Circular tomosynthesis: potential in imaging of breast and upper cervical spine—preliminary phantom and in vitro study. Radiology 2003;228:569-75.

34.Canella C, Philippe P, Pansini V, Salleron J, Flipo RM, Cotten A. Use of tomosynthesis for erosion evaluation in rheumatoid arthritic hands and wrists. Radiology 2011;258:199-205.

35. Duryea J, Dobbins JT, Lynch JA. Digital tomosynthesis of hand joints for arthritis assessment. Med Phys 2003;30:325-33.

36. Hayashi D, Xu L, Roemer FW, et al. Detection of osteophytes and subchondral cysts in the knee with use of tomosynthesis. Radiology 2012;263:206-15.

37.Conaghan PG, Hunter DJ, Maillefert JF, Reichmann WM, Losina E. Summary and recommendations of the OARSI FDA osteoarthritis Assessment of Structural Change Working Group. Osteoarthritis Cartilage 2011;19:606-10.

38.Eckstein F, Wirth W, Nevitt MC. Recent advances in osteoarthritis imaging-the Osteoarthritis Initiative. Nat Rev Rheumatol 2012;8:622-30.

39.Hayashi D, Guermazi A, Hunter DJ. Osteoarthritis year 2010 in review: imaging. Osteoarthritis Cartilage 2011;19:354-60.

40.Hayashi D, Roemer FW, Guermazi A. Osteoarthritis year 2011 in review: imaging in OA - a radiologists' perspective. Osteoarthritis Cartilage 2012;20:207-14.

41.Roemer FW, Guermazi A. Osteoarthritis year 2012 in review: Imaging. Osteoarthritis Cartilage 2012 Jul 20 [Epub ahead of print].

42.Guermazi A, Niu J, Hayashi D, et al. Prevalence of abnormalities in knees detected by MRI in adults without knee osteoarthritis: population based observational study (Framingham Osteoarthritis Study). BMJ 2012;345:e5339.

43.Crema MD, Roemer FW, Marra MD, et al. Articular cartilage in the knee: current MR imaging techniques and applications in clinical practice and research. Radiographics 2011;31:37-61.

44.Hayashi D, Roemer FW, Katur A, et al. Imaging of synovitis in osteoarthritis: current status and outlook. Semin Arthritis Rheum 2011;41:116-30.

45.Roemer FW, Crema MD, Trattnig S, Guermazi A. Advances in imaging of osteoarthritis and cartilage. Radiology 2011;260:332-54.

46.Xu L, Hayashi D, Roemer FW, Felson DT, Guermazi A. Magnetic Resonance Imaging of Subchondral Bone Marrow Lesions in Association with Osteoarthritis. Semin Arthritis Rheum 2012 Apr 25 [pub ahead of print]

47.Englund M, Roemer FW, Hayashi D, Crema MD, Guermazi A. Meniscus pathology, osteoarthritis and the treatment controversy. Nat Rev Rheumatol 2012;8:412-9.

48.Hayashi D, Roemer FW, Dhina Z, et al. Longitudinal assessment of cyst-like lesions of the knee and their relation to radiographic osteoarthritis and MRI-detected effusion and synovitis in patients with knee pain. Arthritis Res Ther 2010;12:R172.

49.Hayashi D, Guermazi A, Kwoh CK, et al. Semiquantitative assessment of subchondral bone marrow edema-like lesions and subchondral cysts of the knee at 3T MRI: A comparison between intermediate-weighted fat-suppressed spin echo and Dual Echo Steady State sequences. BMC Musculoskelet Disord 2011;12:198.

50.Hayashi D, Englund M, Roemer FW, et al. Knee malalignment is associated with an increased risk for incident and enlarging bone marrow lesions in the more loaded compartments: the MOST study. Osteoarthritis Cartilage 2012;20:1227-33.

51.Roemer FW, Felson DT, Wang K, et al. Co-localisation of non-cartilaginous articular pathology increases risk of cartilage loss in the tibiofemoral joint--the MOST study. Ann Rheum Dis 2012 Sep 6. [Epub ahead of print].

52.Crema MD, Roemer FW, Felson DT, et al. Factors associated with meniscal extrusion in knees with or at risk for osteoarthritis: the Multicenter Osteoarthritis study. Radiology. 2012;264:494-503,

53. Roemer FW, Guermazi A, Felson DT, et al. Presence of MRI-detected joint effusion and synovitis increases the risk of cartilage loss in knees without osteoarthritis at 30-month follow-up: the MOST study. Arthritis Rheum. 2012;64:1888-98,

54. Roemer FW, Guermazi A, Felson DT, et al. Presence of MRI-detected joint effusion and synovitis increases the risk of cartilage loss in knees without osteoarthritis at 30-month follow-up: the MOST study.Ann Rheum Dis. 2011;70:1804-9.,

55. Englund M, Felson DT, Guermazi A, et al. Risk factors for medial meniscal pathology on knee MRI in older US adults: a multicentre prospective cohort study. Ann Rheum Dis. 2011;70:1733-9.

56. Roemer FW, Felson DT, Wang K, et al. Co-localisation of non-cartilaginous articular pathology increases risk of cartilage loss in the tibiofemoral joint--the MOST study. Ann Rheum Dis. 2012 Sep 6. [Epub ahead of print]

57. Roemer FW, Guermazi A, Niu J, et al. Prevalence of magnetic resonance imaging-defined atrophic and hypertrophic phenotypes of knee osteoarthritis in a population-based cohort. Arthritis Rheum. 2012;64:429-37

58. Hunter DJ, Arden N, Conaghan P, et al. Definition of osteoarthritis on MRI: results of a Delphi exercise. Osteoarthritis Cartilage. 2011;19:963-9

59. Zhang Y, Nevitt M, Niu J, et al. Fluctuation of knee pain and changes in bone marrow lesions, effusions, and synovitis on magnetic resonance imaging. Arthritis Rheum 2011;63:691-9.

60. Guermazi A, Roemer FW, Hayashi D, et al. Assessment of synovitis with contrast-enhanced MRI using a whole-joint semiquantitative scoring system in people with, or at high risk of, knee osteoarthritis: the MOST study. Ann Rheum Dis 2011;70:805-11.

61. Hunter DJ, Zhang W, Conaghan PG, et al. Systematic review of the concurrent and predictive validity of MRI biomarkers in OA. Osteoarthritis Cartilage 2011;19:557-88.

62. Hunter DJ, Zhang W, Conaghan PG, et al. Responsiveness and reliability of MRI in knee osteoarthritis: a meta-analysis of published evidence. Osteoarthritis Cartilage 2011;19:589-605.

63. Peterfy CG, Guermazi A, Zaim S, et al. Whole-Organ Magnetic Resonance Imaging Score (WORMS) of the knee in osteoarthritis. Osteoarthritis Cartilage 2004;12:177-90.

64. Kornaat PR, Ceulemans RY, Kroon HM, et al. MRI assessment of knee osteoarthritis: Knee Osteoarthritis Scoring System (KOSS)--inter-observer and intraobserver reproducibility of a compartment-based scoring system. Skeletal Radiol 2005;34:95-102.

65. Hunter DJ, Lo GH, Gale D, Grainger AJ, Guermazi A, Conaghan PG. The reliability of a new scoring system for knee osteoarthritis MRI and the validity of bone marrow lesion assessment: BLOKS (Boston Leeds Osteoarthritis Knee Score). Ann Rheum Dis 2008;67:206-11.

66. Lynch JA, Roemer FW, Nevitt MC, et al. Comparison of BLOKS and WORMS scoring systems part I. Cross sectional comparison of methods to assess cartilage morphology, meniscal damage and bone marrow lesions on knee MRI: data from the osteoarthritis initiative. Osteoarthritis Cartilage 2010;18:1393-401.

67.Felson DT, Lynch J, Guermazi A, et al. Comparison of BLOKS and WORMS scoring systems part II. Longitudinal assessment of knee MRIs for osteoarthritis and suggested approach based on their performance: data from the Osteoarthritis Initiative. Osteoarthritis Cartilage 2010;18:1402-7.

68.Roemer FW, Nevitt MC, Felson DT, et al. Predictive validity of within-grade scoring of longitudinal changes of MRI-based cartilage morphology and bone marrow lesion assessment in the tibio-femoral joint - the MOST Study. Osteoarthritis Cartilage 2012 Jul 27 [Epub ahead of print].

69.Katz JN, Chaisson CE, Cole B, et al. The MeTeOR Trial (Meniscal Tear in Osteoarthritis Research): Rationale and design features. Contemp Clin Trials. 2012;33(6):1189-1196

70. Pivotal Osteoarthritis Initiative Magnetic Resonance Imaging Analyses (POMA). Availale at http://www.niams.nih.gov/Funding/Funded_Research/Osteoarthritis_Initiative/pivotal_mri.asp, accessed on October 5th 2012

71. Baker K, Grainger A, Niu J, et al. Relation of synovitis to knee pain using contrast-enhanced MRIs. Ann Rheum Dis 2010;69:1779-83.

72. Loeuille D, Sauliere N, Champigneulle J, Rat AC, Blum A, Chary-Valckenaere I. Comparing non-enhanced and enhanced sequences in the assessment of effusion and synovitis in knee OA: associations with clinical, macroscopic and microscopic features. Osteoarthritis Cartilage 2011;19:1433-9.

73. Grainger AJ, Farrant JM, O'Connor PJ, et al. MR imaging of erosions in interphalangeal joint osteoarthritis: is all osteoarthritis erosive? Skeletal Radiol 2007;36:737-45.

74. Tan AL, Grainger AJ, Tanner SF, Emery P, McGonagle D. A high-resolution magnetic resonance imaging study of distal interphalangeal joint arthropathy in psoriatic arthritis and osteoarthritis: are they the same? Arthritis Rheum 2006;54:1328-33.

75. Tan AL, Grainger AJ, Tanner SF, et al. High-resolution magnetic resonance imaging for the assessment of hand osteoarthritis. Arthritis Rheum 2005;52:2355-65.

76. Tan AL, Toumi H, Benjamin M, et al. Combined high-resolution magnetic resonance imaging and histological examination to explore the role of ligaments and tendons in the phenotypic expression of early hand osteoarthritis. Ann Rheum Dis 2006;65:1267-72.

77. Iagnocco A, Perella C, D'Agostino MA, Sabatini E, Valesini G, Conaghan PG. Magnetic resonance and ultrasonography real-time fusion imaging of the hand and wrist in osteoarthritis and rheumatoid arthritis. Rheumatology (Oxford) 2011;50:1409-13.

78. Schraml C, Schwenzer NF, Martirosian P, et al. Assessment of synovitis in erosive osteoarthritis of the hand using DCE-MRI and comparison with that in its major mimic, the psoriatic arthritis. Acad Radiol 2011;18:804-9.

79.Wittoek R, Jans L, Lambrecht V, Carron P, Verstraete K, Verbruggen G. Reliability and construct validity of ultrasonography of soft tissue and destructive changes in erosive osteoarthritis of the interphalangeal finger joints: a comparison with MRI. Ann Rheum Dis 2011;70:278-83.

80.Haugen IK, Lillegraven S, Slatkowsky-Christensen B, et al. Hand osteoarthritis and MRI: development and first validation step of the proposed Oslo Hand Osteoarthritis MRI score. Ann Rheum Dis 2011;70:1033-8.

81. Slatkowsky-Christensen B, Mowinckel P, Loge JH, Kvien TK. Health-related quality of life in women with symptomatic hand osteoarthritis: a comparison with rheumatoid arthritis patients, healthy controls, and normative data. Arthritis Rheum 2007;57:1404-9.

82. Haugen IK, Boyesen P, Slatkowsky-Christensen B, et al. Comparison of features by MRI and radiographs of the interphalangeal finger joints in patients with hand osteoarthritis. Ann Rheum Dis 2012;71:345-50.

83. Haugen IK, Boyesen P, Slatkowsky-Christensen B, Sesseng S, van der Heijde D, Kvien TK. Associations between MRI-defined synovitis, bone marrow lesions and structural features and measures of pain and physical function in hand osteoarthritis. Ann Rheum Dis 2012;71:899-904.

84. Neumann G, Mendicuti AD, Zou KH, et al. Prevalence of labral tears and cartilage loss in patients with mechanical symptoms of the hip: evaluation using MR arthrography. Osteoarthritis Cartilage 2007;15:909-17.

85. Reichenbach S, Leunig M, Werlen S, et al. Association between cam-type deformities and magnetic resonance imaging-detected structural hip damage: a cross sectional study in young men. Arthritis Rheum 2011;63:4023-30.

86. Potter HG, Schachar J. High resolution noncontrast MRI of the hip. J Magn Reson Imaging 2010;31:268-78.

87. Roemer FW, Hunter DJ, Winterstein A, et al. Hip Osteoarthritis MRI Scoring System (HOAMS): reliability and associations with radiographic and clinical findings. Osteoarthritis Cartilage 2011;19:946-62.

88. Eckstein F, Ateshian G, Burgkart R, et al. Proposal for a nomenclature for magnetic resonance imaging based measures of articular cartilage in osteoarthritis. Osteoarthritis Cartilage 2006;14:974-83.

89. Buck RJ, Wyman BT, Le Graverand MP, Wirth W, Eckstein F. An efficient subset of morphological measures for articular cartilage in the healthy and diseased human knee. Magn Reson Med 2010;63:680-90.

90. Buck RJ, Wyman BT, Le Graverand MP, Hudelmaier M, Wirth W, Eckstein F. Does the use of ordered values of subregional change in cartilage thickness improve the detection of disease progression in longitudinal studies of osteoarthritis? Arthritis Rheum 2009;61:917-24.

91. Buck RJ, Wyman BT, Hellio Le Graverand MP, et al. Using ordered values of subregional cartilage thickness change increases sensitivity in detecting risk factors for osteoarthritis progression. Osteoarthritis Cartilage. 2011;19:302-8.

92. Wirth W, Buck R, Nevitt M, et al. MRI-based extended ordered values more efficiently differentiate cartilage loss in knees with and without joint space narrowing than region-specific approaches using MRI or radiography--data from the OA initiative. Osteoarthritis Cartilage 2011;19:689-99.

93. Ding C, Cicuttini F, Jones G. Do NSAIDs affect longitudinal changes in knee cartilage volume and knee cartilage defects in older adults? Am J Med 2009;122:836-42.

94. Raynauld JP, Martel-Pelletier J, Beaulieu A, et al. An Open-Label Pilot Study Evaluating by Magnetic Resonance Imaging the Potential for a Disease-Modifying Effect of Celecoxib Compared to a Modelized Historical Control Cohort in the Treatment of Knee Osteoarthritis. Semin Arthritis Rheum 2010.

95. Wei S, Venn A, Ding C, et al. The associations between parity, other reproductive factors and cartilage in women aged 50-80 years. Osteoarthritis Cartilage 2011;19:1307-13.

96. Intema F, Van Roermund PM, Marijnissen AC, et al. Tissue structure modification in knee osteoarthritis by use of joint distraction: an open 1-year pilot study. Ann Rheum Dis. 2011;70:1441-6.

97. Bennell KL, Bowles KA, Wang Y, Cicuttini F, Davies-Tuck M, Hinman RS. Higher dynamic medial knee load predicts greater cartilage loss over 12 months in medial knee osteoarthritis. Ann Rheum Dis 2011;70:1770-4.

98. Eckstein F, Cotofana S, Wirth W, et al. Greater rates of cartilage loss in painful knees than in pain-free knees after adjustment for radiographic disease stage: data from the osteoarthritis initiative. Arthritis Rheum 2011;63:2257-67.

99. Eckstein F, Wirth W, Hudelmaier MI, et al. Relationship of compartment-specific structural knee status at baseline with change in cartilage morphology: a prospective observational study using data from the osteoarthritis initiative. Arthritis Res Ther 2009;11:R90.

100. Eckstein F, Nevitt M, Gimona A, et al. Rates of change and sensitivity to change in cartilage morphology in healthy knees and in knees with mild, moderate, and end-stage

radiographic osteoarthritis: results from 831 participants from the Osteoarthritis Initiative. Arthritis Care Res (Hoboken). 2011;63:311-9.

101. Cotofana S, Buck R, Wirth W, et al. Cartilage thickening in early radiographic human knee osteoarthritis - within-person, between-knee comparison. Arthritis Care Res (Hoboken) 2012 May 3 [Epub ahead of print].

102. Frobell RB, Nevitt MC, Hudelmaier M, et al. Femorotibial subchondral bone area and regional cartilage thickness: a cross-sectional description in healthy reference cases and various radiographic stages of osteoarthritis in 1,003 knees from the Osteoarthritis Initiative. Arthritis Care Res (Hoboken). 2010;62:1612-23.

103. Eckstein F, Kwoh CK, Boudreau RM, et al. Quantitative MRI measures of cartilage predict knee replacement: a case-control study from the Osteoarthritis Initiative. Ann Rheum Dis 2012 Jun 23 [Epub ahead of print].

104. Eckstein F, Mc Culloch CE, Lynch JA, et al. How do short-term rates of femorotibial cartilage change compare to long-term changes? Four year follow-up data from the osteoarthritis initiative. Osteoarthritis Cartilage 2012;20:1250-7.

105. Schneider E, Nevitt M, McCulloch C, et al. Equivalence and precision of knee cartilage morphometry between different segmentation teams, cartilage regions, and MR acquisitions. Osteoarthritis Cartilage 2012;20:869-79.

106. Sitoci KH, Hudelmaier M, Eckstein F. Nocturnal changes in knee cartilage thickness in young healthy adults. Cells, tissues, organs 2012;196:189-94.

107. Cotofana S, Eckstein F, Wirth W, et al. In vivo measures of cartilage deformation: patterns in healthy and osteoarthritic female knees using 3T MR imaging. Eur Radiol. 2011;21:1127-35.

108. Niehoff A, Müller M, Brüggemann L, et al. Deformational behaviour of knee cartilage and changes in serum cartilage oligomeric matrix protein (COMP) after running and drop landing. Osteoarthritis Cartilage. 2011;19:1003-10.

109. Wirth W, Frobell RB, Souza RB, et al. A three-dimensional quantitative method to measure meniscus shape, position, and signal intensity using MR images: a pilot study and preliminary results in knee osteoarthritis. Magn Reson Med 2010;63:1162-71.

110. Siorpaes K, Wenger A, Bloecker K, et al. Interobserver reproducibility of quantitative meniscus analysis using coronal multiplanar DESS and IWTSE MR imaging. Magn Reson Med. 2012;67:1419-26.

111. Bloecker K, Englund M, Wirth W, et al. Size and position of the healthy meniscus, and its correlation with sex, height, weight, and bone area- a cross-sectional study. BMC Musculoskelet Disord. 2011;28;12:248.

112. Swanson MS, Prescott JW, Best TM, et al. Semi-automated segmentation to assess the lateral meniscus in normal and osteoarthritic knees. Osteoarthritis Cartilage 2010;18:344-53.

113. Wenger A, Englund M, Wirth W, et al. Relationship of 3D meniscal morphology and position with knee pain in subjects with knee osteoarthritis: a pilot study. Eur Radiol 2012;22:211-20.

114. Roemer FW, Khrad H, Hayashi D, et al. Volumetric and semiquantitative assessment of MRI-detected subchondral bone marrow lesions in knee osteoarthritis: a comparison of contrast-enhanced and non-enhanced imaging. Osteoarthritis Cartilage 2010;18:1062-6.

115. Driban JB, Lo GH, Lee JY, et al. Quantitative bone marrow lesion size in osteoarthritic knees correlates with cartilage damage and predicts longitudinal cartilage loss. BMC Musculoskelet Disord 2011;12:217.

116. Fotinos-Hoyer AK, Guermazi A, Jara H, et al. Assessment of synovitis in the osteoarthritic knee: Comparison between manual segmentation, semi-automated segmentation and semiquantitative assessment using contrast-enhanced fat-suppressed T1-weighted MRI. Magn Reson Med 2010;64:604-9.

117. Habib S, Guermazi A, Ozonoff A, et al. MRI-based volumetric assessment of joint effusion in knee osteoarthritis using proton density-weighted fat-suppressed and T1-weighted contrast-enhanced fat-suppressed sequences. Skeletal Radiol. 2011;40:1581-5.

118. Burstein D, Gray M, Mosher T, et al. Measures of molecular composition and structure in osteoarthritis. Radiol Clin N Am. 2009;47:675-86.

119. Crema MD, Roemer FW, Marra MD, et al. Articular cartilage in the knee: current MR imaging techniques and applications in clinical practice and research. Radiographics 2011;31:37-61.

120. McAlindon TE, Nuite M, Krishnan N, et al. Change in knee osteoarthritis cartilage detected by delayed gadolinium enhanced magnetic resonance imaging following treatment with collagen hydrolysate: a pilot randomized controlled trial. Osteoarthritis Cartilage 2011;19:399-405.

121. Van Ginckel A, Baelde N, Almqvist KM, et al. Functional adaptation of knee cartilage in asymptomatic female novice runners compared to sedentary controls. A longitudinal analysis using delayed Gadolinium Enhanced Magnetic Resonance Imaging of Cartilage (dGEMRIC). Osteoarthritis Cartilage 2010;18:1564-9.

122. Souza RB,Stehling C, Wyman BT, et al. The effects of acute loading on T1rho and T2 relaxation times of tibiofemoral articular cartilage. OAC 2010;18:1557-63.

123. Hovis KK, Stehling C,Souza RB, et al. Physical activity is associated with magnetic resonance imaging-based knee cartilage T2 measurements in asymptomatic subjects with and those without osteoarthritis risk factors. Arthritis Rheum 2011;63:2248-56.

124. Pan J, Pialat JB, Joseph T, et al. Knee cartilage T2 characteristics and evolution in relation to morphologic abnormalities detected at 3-T MR imaging: a longitudinal study of the normal control cohort from the Osteoarthritis Initiative. Radiology 2011;261:507-15.

125. Anandacoomarasamy A, Leibman S, Smith G, et al. Weight loss in obese people has structure-modifying effects on medial but not on lateral knee articular cartilage. Ann Rheum Dis 2012;71:26-32.

126. Williams A, Qian Y, Golla S, et al. UTE-T2∗ mapping detects sub-clinical meniscus injury after anterior cruciate ligament tear. Osteoarthritis Cartilage 2012;20:486-94.

127. Raya JG, Horng A, Dietrich O, et al. Articular cartilage: in vivo diffusion-tensor imaging. Radiology 2012;262:550-9.

128. Madelin G, Babb JS, Xia D, et al. Reproducibility and repeatability of quantitative sodium magnetic resonance imaging in vivo in articular cartilage at 3 T and 7 T. Magn Reson Med 2012;68:841-9

129. Newbould RD, Miller SR, Tielbeek JA, et al. Reproducibility of sodium MRI measures of articular cartilage of the knee in osteoarthritis. Osteoarthritis Cartilage 2012;20:29-35

130. Newbould RD, Miller SR, Toms LD, et al. T2* measurement of the knee articular cartilage in osteoarthritis at 3T. J Magn Reson Imaging. 2012;35:1422-9

131. Keen HI, Conaghan PG. Ultrasonography in osteoarthritis. Radiol Clin N Am 2009;47:581-94.

132. Wakefield RJ, Gibbon WW, Conaghan PG, et al. The value of sonography in the detection of bone erosions in patients with rheumatoid arthritis: a comparison with conventional radiography. Arthritis Rheum 2000;43:2762-70.

133. Wakefield RJ, Balint P, Szkudlarek M, et al. Musculoskeletal ultrasound including definitions for ultrasonographic pathology. J Rheumatol 2005;32:2485-7.

134. Keen HI, Lavie F, Wakefield RJ, et al. The development of a preliminary ultrasonographic scoring system for features of hand osteoarthritis. Ann Rheum Dis 2008;67:651-5.

135. Kortekaas MC, Kwok WY, Reijnierse M, et al. Osteophytes and joint space narrowing are independently associated with pain in finger joints in hand osteoarthritis. Ann Rheum Dis 2011;70:1835-7.

136. Kortekaas MC, Kwok WY, Reijnierse M, et al. In erosive hand osteoarthritis more inflammatory signs on ultrasound are found than in the rest of hand osteoarthritis. Ann Rheum Dis 2012 Jul 20. [Epub ahead of print].

137. Klauser AS, Faschingbauer R, Kupferthaler K, et al. Sonographic criteria for therapy follow-up in the course of ultrasound-guided intra-articular injections of hyaluronic acid in hand osteoarthritis. Eur J Radiol 2012;81:1607-11.

138. Conaghan PG, D'Agostino MA, Le Bars M, et al. Clinical and ultrasonographic predictors of joint replacement for knee osteoarthritis: results from a large, 3-year, prospective EULAR study. Ann Rheum Dis 2010;69:644-7.

139. Kumm J, Tamm A, Lintrop M, et al. Association between ultrasonographic findings and bone/cartilage biomarkers in patients with early-stage knee osteoarthritis. Calcif Tissue Int 2009;85:514-22.

140. Saarakkala S, Waris P, Waris V, et al. Diagnostic performance of knee ultrasonography for detecting degenerative changes of articular cartilage. Osteoarthritis Cartilage 2012;20:376-81.

141. Kawaguchi K, Enokida M, Otsuki R, et al. Ultrasonographic evaluation of medial radial displacement of the medial meniscus in knee osteoarthritis. Arthritis Rheum 2012;64:173-80.

142. Chao J, Wu C, Sun B, et al. Inflammatory characteristics on ultrasound predict poorer longterm response to intraarticular corticosteroid injections in knee osteoarthritis. J Rheumatol 2010;37:650-5.

143. Wu PT, Shao CJ, Wu KC, et al. Pain in patients with equal radiographic grades of osteoarthritis in both knees: the value of gray scale ultrasound. Osteoarthritis Cartilage 2012 Sep 1. [Epub ahead of print].

144. Omoumi P, Mercier GA, Lecouvet F, et al. CT arthrography, MR arthrography, PET and scintigraphy in osteoarthritis. Radiol Clin N Am 2009;47:595-615.

145. Nakamura H, Masuko K, Yudoh K, et al. Positron emission tomography with 18F-FDG in osteoarthritic knee. Osteoarthritis Cartilage 2007;15:673-81.

146. Umemoto Y, Oka T, Inoue T, et al. Imaging of a rat osteoarthritis model using (18)F-fluoride positron emission tomography. Ann Nucl Med 2010;24:663-9.

147. Temmerman OP, Raijmakers PG, Kloet R, et al. In vivo measurements of blood flow and bone metabolism in osteoarthritis. Rheumatol Int 2012 Jul 26 [Epub ahead of print].

148. Cachin F, Boisgard S, Vidal A, et al. First ex vivo study demonstrating that 99mTc-NTP 15-5 radiotracer binds to human articular cartilage. Eur J Nucl Med Mol Imaging 2011;38:2077-82.

149. Moon YL, Lee SH, Park SY, Yu JC, et al. Evaluation of shoulder disorders by 2-[F-18]-fluoro-2-deoxy-D-glucose positron emission tomography and computed tomography. Clin Orthop Surg 2010;2:167-72.

150. Magee D, Tanner SF, Waller M, Tan et al. Combining variational and model-based techniques to register PET and MR images in hand osteoarthritis. Phys Med Biol 2010;55:4755-69.

151. Naviscan. Naviscan high-resolution PET scanner. Available at: http://www.naviscan.com/products/product-overview/product-overview. Accessed October 1, 2012.

152. Hechelhammer L, Pfirmann CW, Zanetti M, et al. Imaging findings predicting the outcome of cervical facet joint blocks. Eur Radiol 2007;17:959-64.

153. Kalichman L, Li L, Kim DH, et al. Facet joint osteoarthritis and low back pain in the community-based population. Spine 2008;33:2560-5.

154. Kalichman L, Kim DH, Li L, et al. Computed tomography evaluated features of spinal degeneration: prevalence, intercorrelation, and association with self-reported low back pain. Spine 2010;10:200-8.

155. Suri P, Katz JN, Rainville J, et al. Vascular disease is associated with facet joint osteoarthritis. Osteoarthritis Cartilage 2010;18:1127-32.

156. Kalichman L, Guermazi A, Li L, et al. Association between age, sex, BMI and CT-evaluated spinal degeneration features. J Back Musculoskelet Rehabil 2009;22:189-95.

157. Kim JS, Kroin JS, Buvanendran A, et al. Characterization of a new animal model for evaluation and treatment of back pain due to lumbar facet joint osteoarthritis. Arthritis Rheum 2011;63:2966-73.

158. Hall FM, Goldberg RP, Wyshak G, et al. Shoulder arthrography: comparison of morbidity after use of various contrast media. Radiology 1985;154:339-41.

159. Andreisek G, Froehlich JM, Hodler J, et al. Direct MR arthrography at 1.5 and 3.0 T: signal dependence on gadolinium and iodine concentrations--phantom study. Radiology 2008;247:706-16.

160. Brown RR, Clarke DW, Daffner RH. Is a mixture of gadolinium and iodinated contrast material safe during MR arthrography? AJR Am J Roentgenol 2000;175:1087-90.

161. Berquist TH. Imaging of articular pathology: MRI, CT, arthrography. Clinical anatomy 1997;10:1-13.

162. El-Khoury GY, Alliman KJ, Lundberg HJ, et al. Cartilage thickness in cadaveric ankles: measurement with double-contrast multi-detector row CT arthrography versus MR imaging. Radiology 2004;233:768-73.

163. Wyler A, Bousson V, Bergot C, et al. Hyaline cartilage thickness in radiographically normal cadaveric hips: comparison of spiral CT arthrographic and macroscopic measurements. Radiology 2007;242:441-9.

164. Wyler A, Bousson V, Bergot C, et al. Comparison of MR-arthrography and CT arthrography in hyaline cartilage-thickness measurement in radiographically normal cadaver hips with anatomy as gold standard. Osteoarthritis Cartilage 2009;17:19-25.

165. Schmid MR, Pfirrmann CW, Hodler J, et al. Cartilage lesions in the ankle joint: comparison of MR arthrography and CT arthrography. Skeletal Radiol 2003;32:259-65.

166. McCauley TR, Kornaat PR, Jee WH. Central osteophytes in the knee: prevalence and association with cartilage defects on MR imaging. AJR Am J Roentgenol 2001;176:359-64.

167. Kraniotis P, Maragkos S, Tyllianakis M, et al. Ankle posttraumatic osteoarthritis: a CT arthrography study in patients with bi- and trimalleolar fractures. Skeletal Radiol 2012;41:803-9.

168. Tamura S, Nishii T, Shiomi T, et al. Three-dimensional patterns of early acetabular cartilage damage in hip dysplasia; a high-resolutional CT arthrography study. Osteoarthritis Cartilage. 2012;20:646-52.

Figures

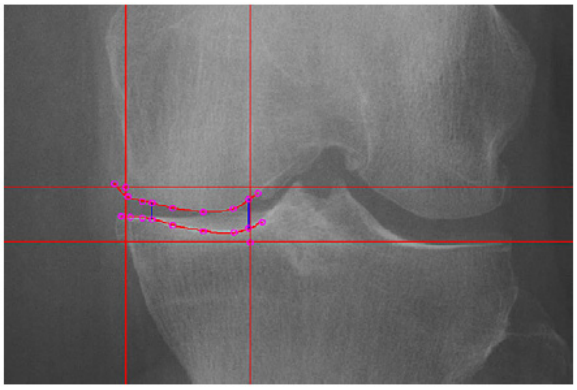

Figure 1. Automated computer measurement of JSW of the medial tibial plateau of the knee. Minimum JSW is measured using software (Holy's software, Claude Bernard University, Lyon, France) in which the joint space contour is automatically delineated by the computer with the help of an edge-based algorithm. The area of measurement of minimum JSW is defined by two vertical lines and two horizontal lines obtained by a single click on the non osteophytic outer edge of the medial femoral condyle and a single click on the inner edge of the medial tibial plateau close to the articular surface. Within these landmarks, the delineation of the bone edges of the medial femoral condyle and medial tibial plateau floor, in addition to the minimum JSW, are automatically obtained.

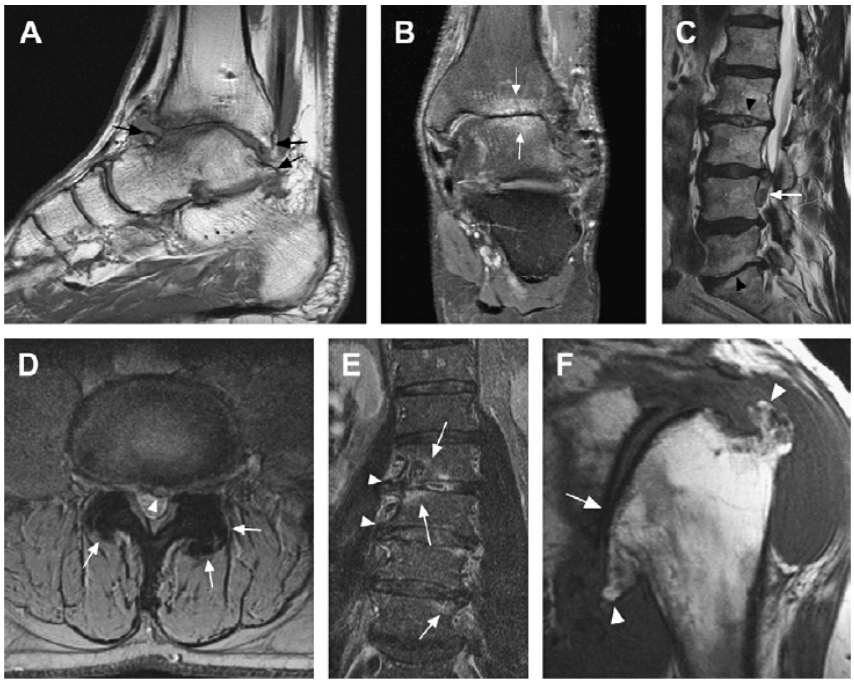

Figure 2. Examples of 1.5-T MR imaging of advanced OA. (A) Sagittal T1-weighted MR image of post traumatic ankle OA shows large periarticular osteophytes (arrows). (B) Coronal T2-weighted fat-suppressed MR image shows periarticular subchondral BMLs (white arrows). (C) Sagittal T2- weighted MR image of lumbar spine OA shows disc space narrowing at L2 to L3 and at L5 to S1 (arrowheads). There is an additional inferiorly displaced disc herniation at L3 to L4 (white arrow). (D) Axial T2-weighted gradient-echo MR image at the level of L3 to L4 shows hypertrophic facet joint OA (white arrows) and a small medial disc herniation (arrowhead). (E) Coronal short tau inversion recovery (STIR) MR image of the lumbar spine demonstrates peridiscal edema-like lesions at L2 to L3 and at L4 to L5 (arrows). Note the peridiscal lateral osteophytes (arrowheads). (F) Sagittal T1-weighted MR image of advanced shoulder OA shows large humeral osteophytes (arrowheads) and severe JSN and cartilage loss (arrow).

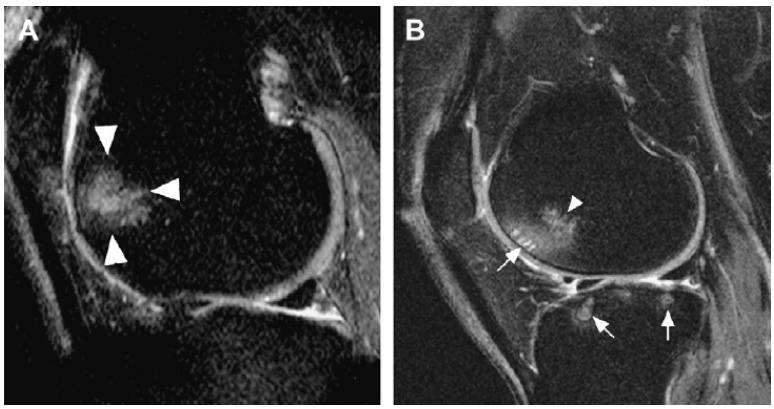

Figure 3. Examples of 1.0 T and 3.0 T MR imaging of knee OA. (A) Sagittal proton density-weighted fat-suppressed 1.0 T MR image shows a subchondral BML in the anterior medial femur (arrowheads) associated with superficial cartilage damage. (B) Sagittal proton density-weighted fat-suppressed 3.0 T MR image shows a subchondral BML in the anterior lateral femur (arrowhead) and femoral and tibial subchondral cysts (arrows).

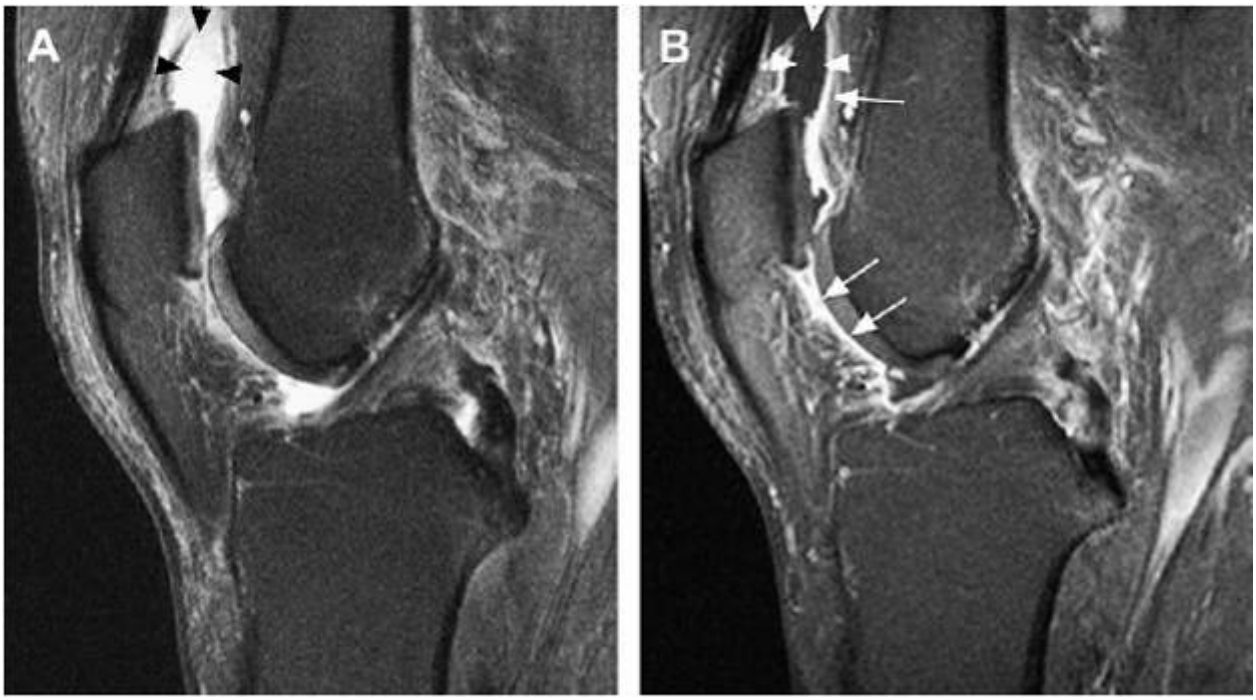

Figure 4. Synovial activation in knee OA. (A) Sagittal proton density-weighted fat-suppressed MR image shows joint effusion depicted as fluid-equivalent signal in the articular cavity (black arrowheads). (B) Sagittal T1-weighted fat-suppressed contrast-enhanced MR image of the same knee shows joint effusion depicted as hypointense signal within the articular cavity (white arrowheads). Supra- and infrapatellar synovial thickening is visualized (white arrows). Note that the true extent of synovial thickening can only be appreciated on T1-weighted contrast-enhanced MR images.

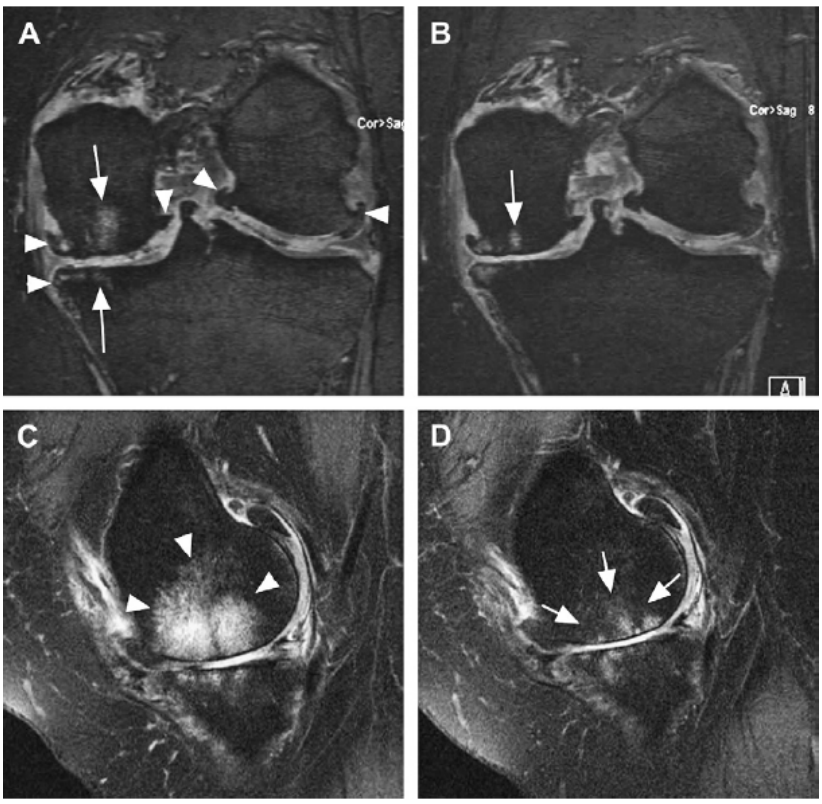

Figure 5. Longitudinal semiquantitative assessment of knee OA. (A) Baseline coronal double echo steady state (DESS) MR image shows central osteophytes scored for the medial and lateral compartments (arrowheads). Subchondral BMLs are shown (arrows). (B) MR image at 12 month follow-up shows increasing cartilage loss in the medial compartment but a decrease of the periarticular BMLs (arrow). The size of the osteophytes has not changed. (C) Sagittal proton density-weighted fat-suppressed MR image demonstrates a large BML in the central weight-bearing part of the medial femur (arrowheads). (D) MR image at 12 month follow-up shows a decrease in the size and signal intensity of the BML (arrows). Note that the BML is better depicted on the spin-echo images (C, D) than on the gradient-echo images (A, B).

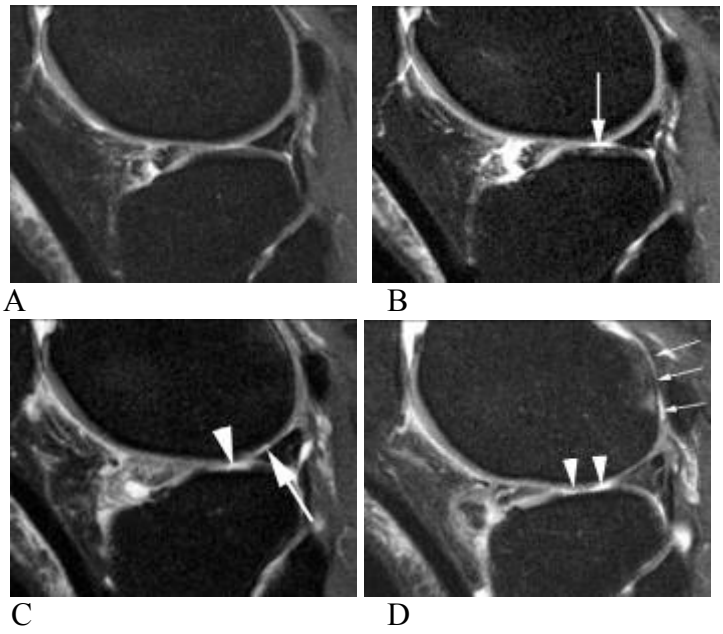

Figure 6. Development of cartilage damage in early osteoarthritis. A. Sagittal intermediate-weighted fat-saturated image shows regular articular chondral surface without focal or diffuse cartilage damage. B. 12 month follow-up image of the same knee at the identical section shows early intrachondral degeneration reflected as hyperintensity within the central weight bearing region of the tibial cartilage but not altering the articular surface (arrow). C. 24 month examination depicts focal full thickness cartilage defect reaching the subchondral plateau at the same location (arrowhead). In addition there is incident superficial cartilage damage at the central part of the lateral femoral condyle adjacent to the posterior horn of the lateral meniscus. D. 36 month follow-up image shows progression to wide spread full thickness cartilage loss in the central weight bearing part of the lateral tibia (arrowheads). In addition there is incident full thickness damage at the posterior aspect of the lateral femoral condyle (thin arrows). Note adjacent BML, which often accompany cartilage damage.

A B C

Figure 7. Progression of meniscal damage over time. A. Sagittal intermediate-weighted fat-saturated image shows intrameniscal high signal representing mucoid degeneration (arrow) in the posterior horn of the medial meniscus that does not reach the meniscal surface. No tear is seen and there is no signal change in the anterior horn. B. 12 month follow-up examination depicts development of the horizontal-oblique tear in the posterior horn. Meniscal hyperintensity now reaches the meniscal undersurface (arrowhead). In addition there is incident mucoid degeneration in the anterior horn (arrow). C. At 36 month follow-up an incident horizontal tear in the anterior horn is seen. In addition meniscal cysts communicating with horizontal tears of the anterior horn (arrowhead) and posterior horn (thick arrow) are visible. Note the subchondral BML adjacent to the full thickness cartilage damage in the posterior aspect of the lateral tibial plateau. (thin arrow).

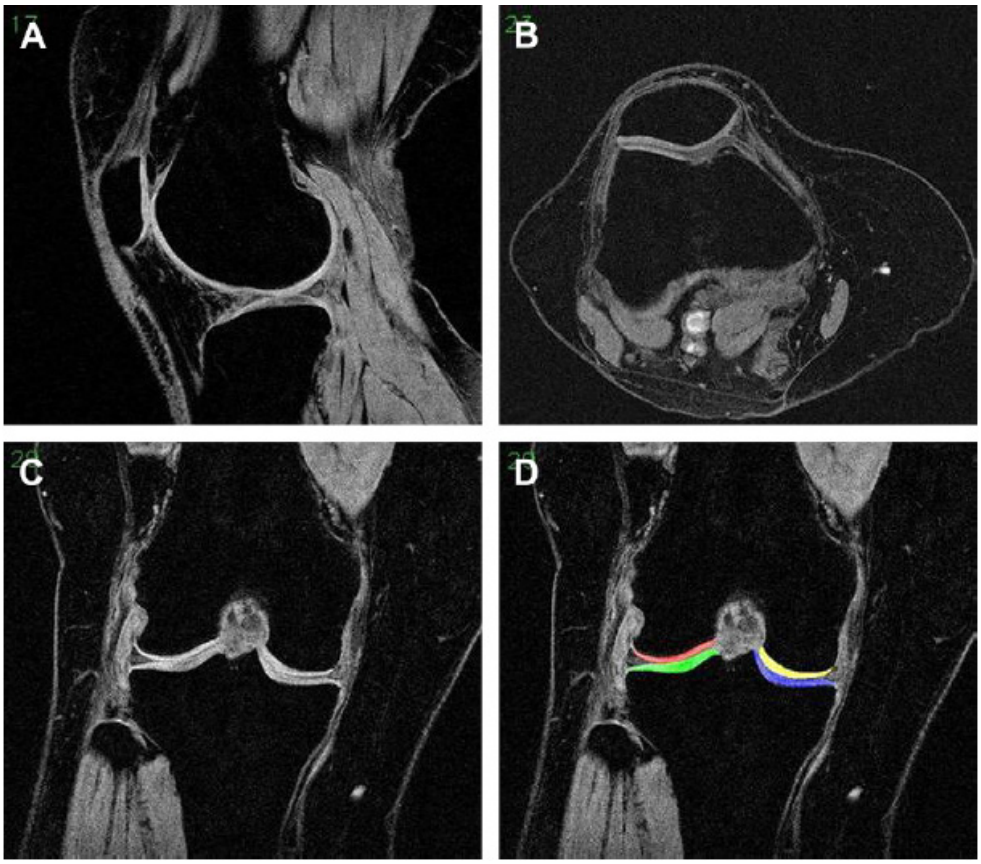

Figure 8. Knee MR image obtained with spoiled gradient-echo (SPGR) sequences with water excitation, in the same person: (A) sagittal image; (B) axial image; (C) coronal image; (D) same coronal image with the medial tibial cartilage marked (segmented) blue, medial femoral cartilage marked yellow, lateral tibial cartilage marked green, and lateral femoral cartilage marked red.

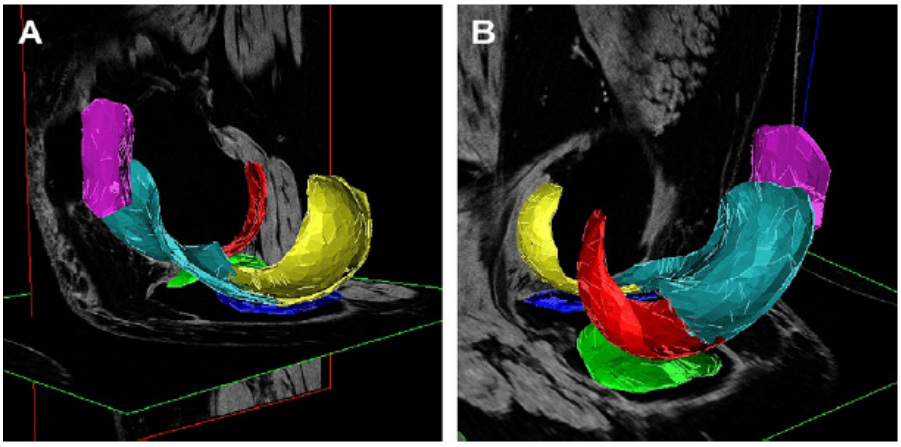

Figure 9. (A, B) 3D reconstruction and visualization of knee cartilage plates from a sagittal MR imaging data set: medial tibial cartilage marked blue, medial femoral cartilage marked yellow, lateral tibial cartilage marked green, lateral femoral cartilage marked red, femoral trochlear cartilage marked turquoise, and patellar cartilage marked magenta.

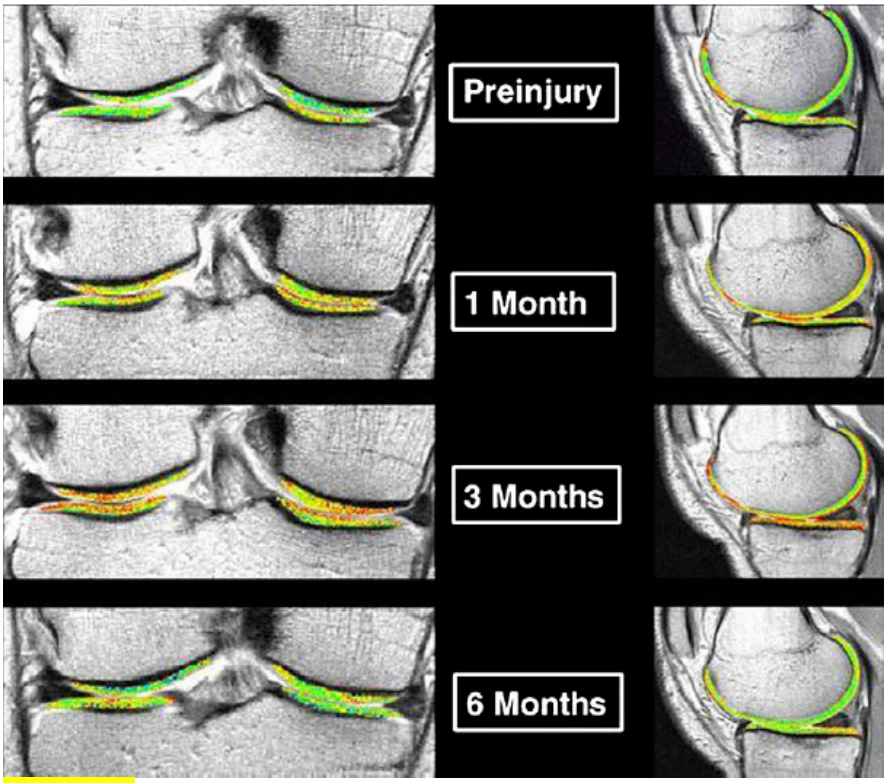

Figure 10. Case study of dGEMRIC as a function of time before and after PCL injury. A decline in the dGEMRIC Index is apparent at one month, with a further decrease at three months and recovery at six months. These data illustrate the potential for biochemical monitoring of cartilage to demonstrate degeneration and recovery of the tissue from a traumatic injury. Similar studies might be used to monitor cartilage status improvement with other mechanical, surgical, or pharmaceutical interventions. (From Young AA, Stanwell P, Williams A, et al. Glycosaminoglycan content of knee cartilage following posterior cruciate ligament rupture demonstrated by delayed gadolinium-enhanced magnetic resonance imaging of cartilage (dGEMRIC). A case report. J Bone Joint Surg Am 2005;87:2765; with permission.)

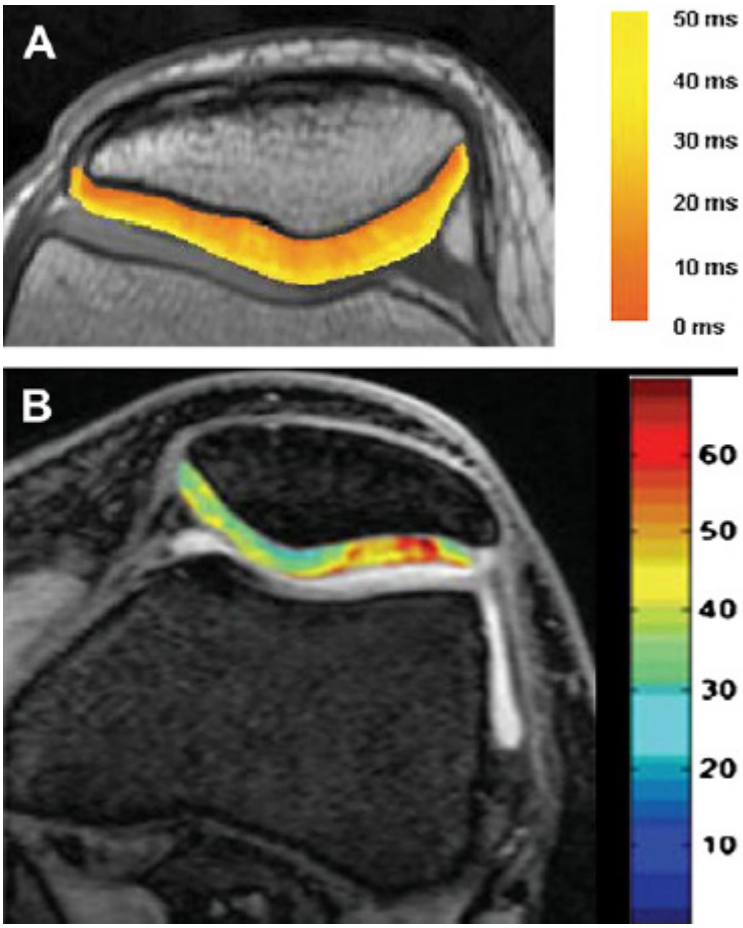

Figure 11. (A) T2 map of patellar cartilage shows variation with cartilage depth. (From Maier CF, Tan SG, Hariharan H, et al. T2 quantitation of articular cartilage at 1.5 T. J Magn Reson Imaging 2003;17:363; with permission.) (B) T1 rho map of patellar cartilage demonstrates a lesion in cartilage that is morphologically thick and intact. (From Borthakur A, Mellon E, Niyogi S, et al. Sodium and T1 rho MRI for molecular and diagnostic imaging of articular cartilage. NMR Biomed 2006;19:799; with permission.) The variation and lesions apparent in maps of these parameters across morphologically intact cartilage enable monitoring of biochemical changes in cartilage before morphologic changes become apparent.

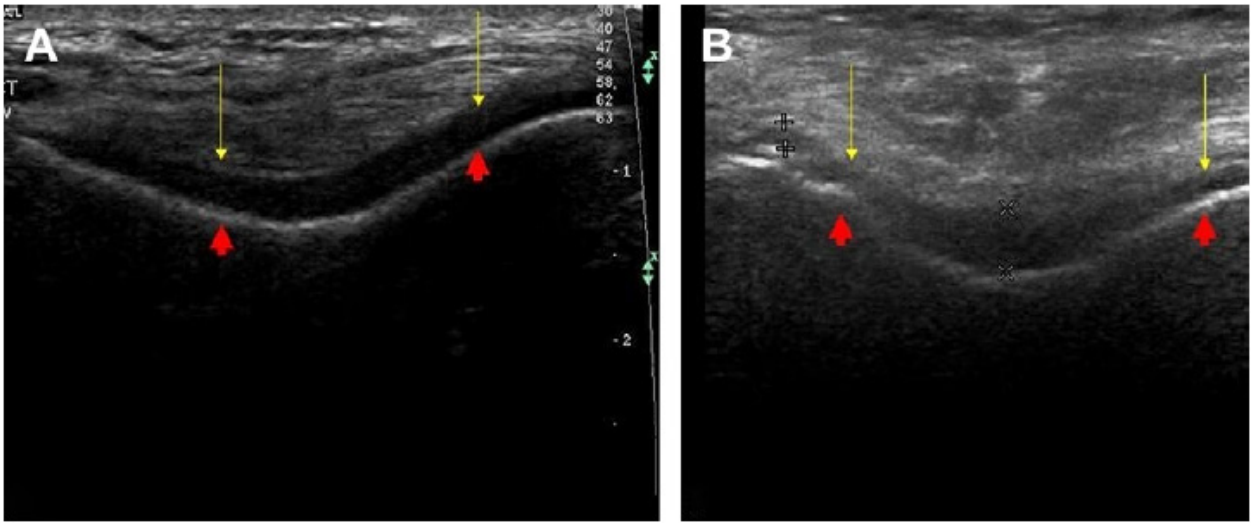

Figure12. OA of the knee. Coronal ultrasound scans through the distal femur of a normal knee (A) and an osteoarthritic knee (B) demonstrate the intracondylar notch. The red arrows indicate the cortical surface of the femur, and the yellow arrows indicate the superficial surface of the cartilage. Note that compared with the normal knee, the cartilage in the osteoarthritic knee is more echoic, there is loss of definition of the margins, and it appears thinner laterally.

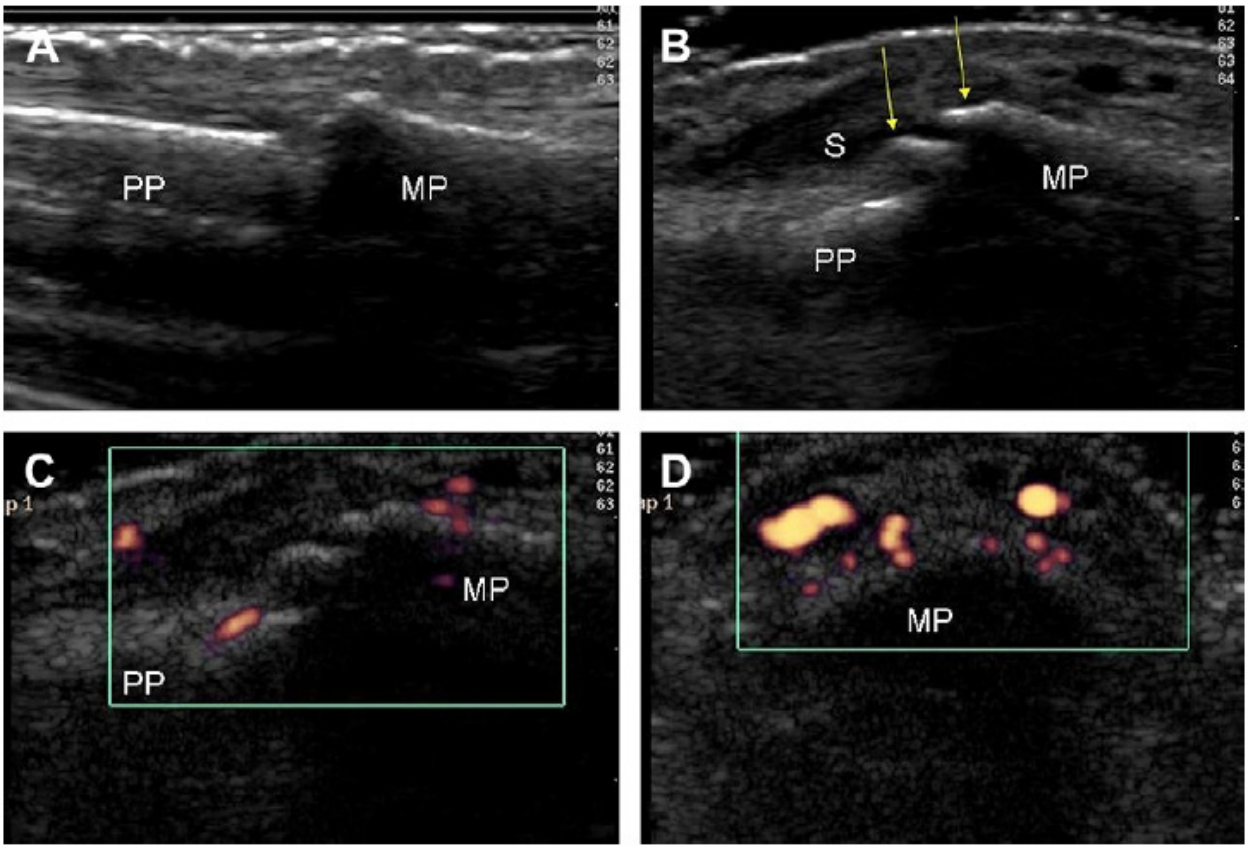

Figure 13. OA of the proximal interphalangeal (PIP) joint. (A) Dorsal longitudinal ultrasound image of a normal PIP joint, with smooth cortical outlines. (B) Dorsal longitudinal ultrasound scan of osteoarthritic PIP joint demonstrates proximal and distal dorsal osteophytes (yellow arrows) and synovial hypertrophy (dark area indicated by an S). Dorsal longitudinal (C) and transverse (D) ultrasound scans of the PIP joint shown in B, with power Doppler function added, demonstrate Doppler signal within the hypoechoic synovial hypertrophy. PP, proximal phalanx; MP, middle phalanx.

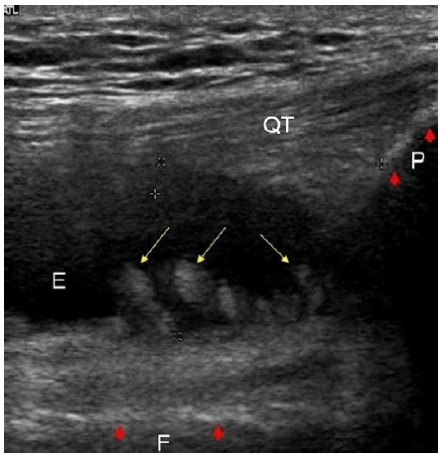

Figure 14. OA in the knee. A longitudinal ultrasound image through the suprapatellar pouch demonstrates synovial hypertrophy with villi formation (yellow arrows) and an effusion (E). The cortical surface of the femur (F) and patella (P) are indicated by the red arrows, and the quadriceps tendon (QT) is also shown.

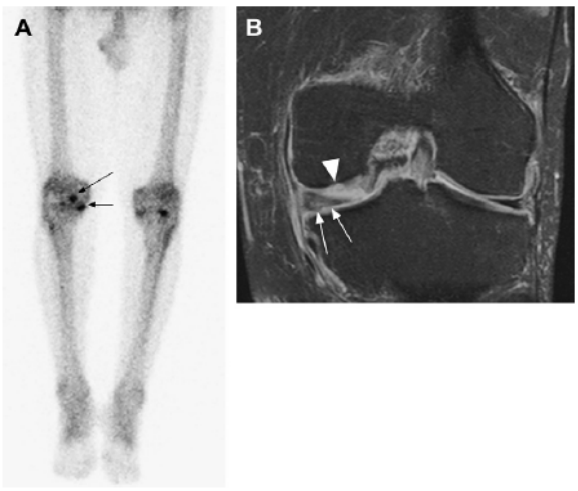

Figure 15. Scintigraphy. (A) Radionuclide accumulation is observed in the medial compartment of the left knee (black arrows) in a patient who has prostate cancer and a high risk for bone metastases. This appearance is nonspecific and more likely secondary to degenerative disease. (B) Coronal T2-weighted fat-suppressed MR image of the same knee shows meniscal degeneration (white arrows) and cartilage damage (arrowhead). The image confirms normal bone marrow without metastatic deposits. (Image courtesy of G. Mercier, MD, PhD, Boston, MA. Reproduced from Guermazi et al. Rheum Dis Clin North Am 2008; 645-687.)

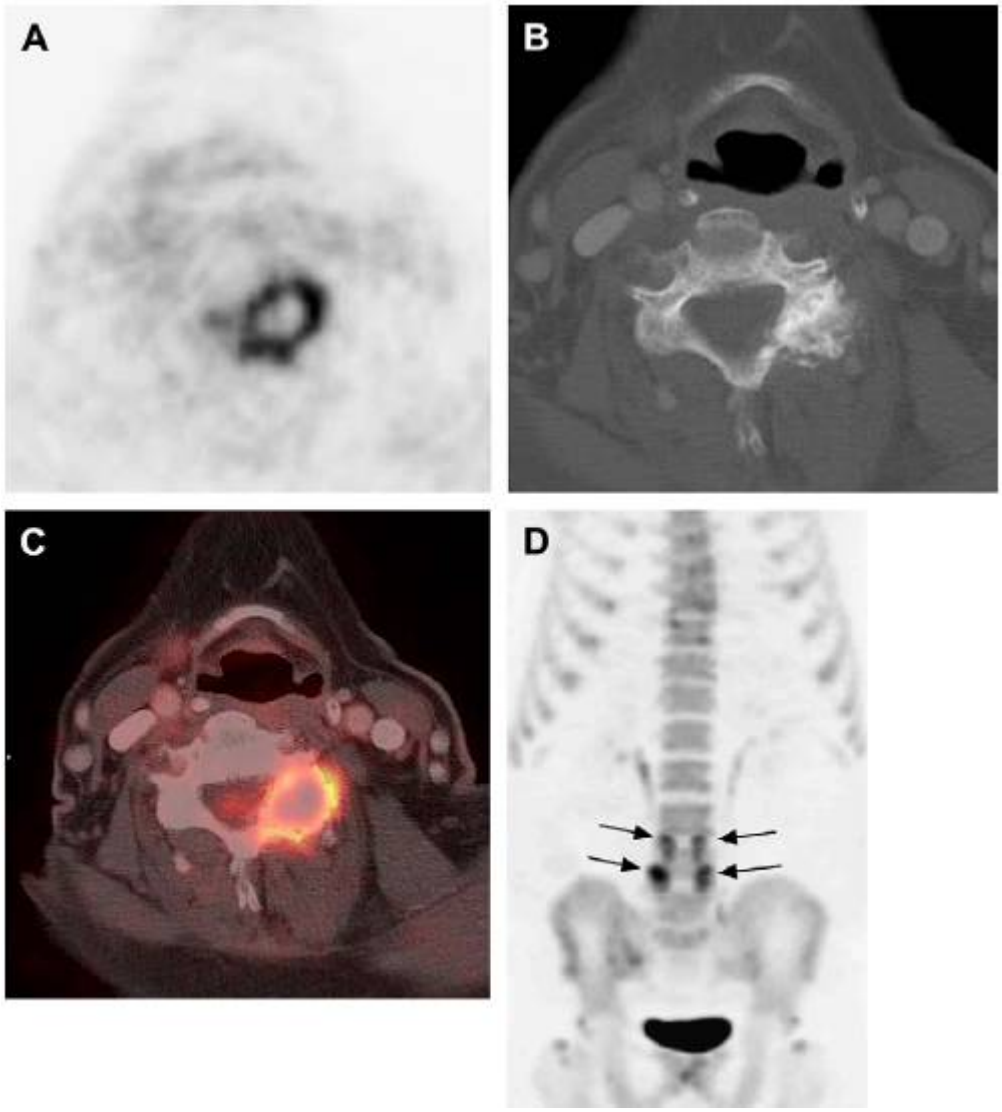

Figure 16. FDG-PET of the cervical spine in a patient who has breast cancer. (A) Axial view FDG-PET shows inflammatory facet joint of the cervical spine OA with strong glucose accumulation around the left facet joint. Note the low spatial resolution of PET. (B) Axial CT shows hypertrophic left-sided facet joint and confirms the osteoarthritic nature of the lesion. (C) Fused PET-CT image superiorly demonstrates the correlation between metabolic changes depicted by PET and spatial localization by CT. (D) Coronal view FDG-PET in the same patients shows bilateral facet joint OA at L4 to L5 and L5 to S1 (arrows). (Image courtesy of G. Mercier,

MD, PhD, Boston, MA. Reproduced from Guermazi et al. Rheum Dis Clin North Am 2008; 645-687.)

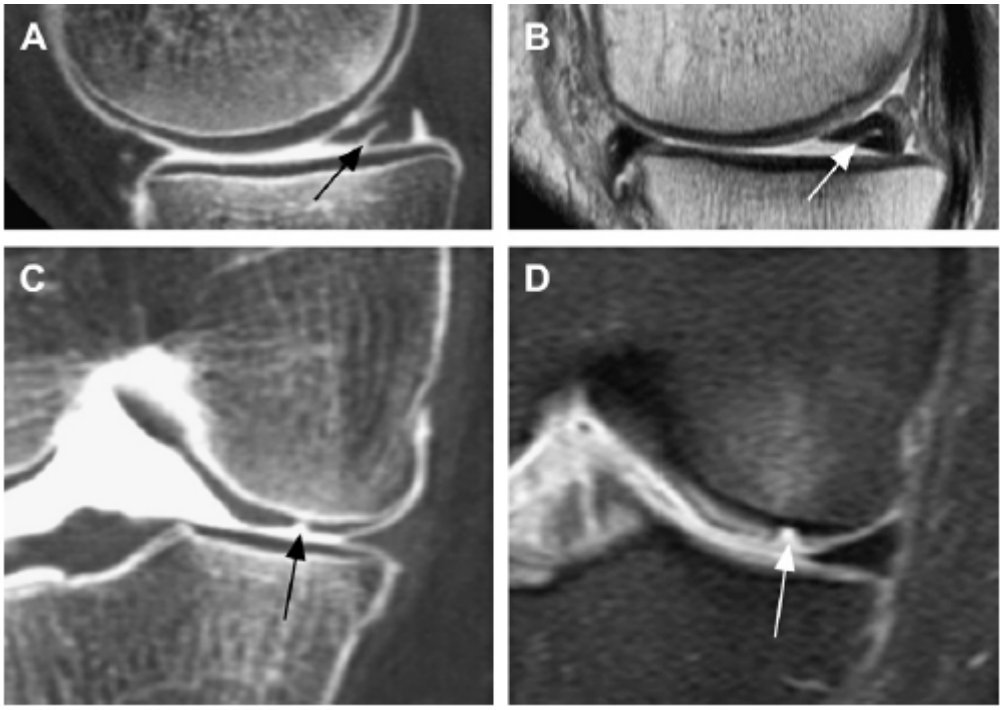

Figure 17. Correlation of CT arthrography and MR imaging. (A) Sagittal reformatted CT arthrography of the medial knee compartment shows posterior horn meniscal tear (arrow). Note superficial cartilage thinning at the femoral condyle adjacent to the meniscus. (B) Sagittal proton density-weighted MR image of the same knee demonstrates the posterior horn meniscal tear (arrow). (C) Coronal reformatted CT arthrography of the medial compartment shows focal cartilage defect in the central femoral condyle (arrow). (D) Coronal fat-suppressed T2-weighted MR image shows the same defect (arrow). (Image courtesy of B. Van de Berg, MD, PhD, Brussels, Belgium. Reproduced from Guermazi et al. Rheum Dis Clin North Am 2008; 645-687.)

Table 1. Comparison of MR imaging features scored by the four semiquantitative MR imaging scoring systems

MRI features	BLOKS	WORMS	MOAKS	KOSS
Cartilage	Uses two scores. Score 1: subregional approach A. % of any cartilage loss in subregion B. % of full-thickness cartilage loss in subregion Score2: site-specific approach. Scoring of cartilage thickness at 11 specific locations (not subregions) from 0 (none) to 2 (full thickness loss)	Subregional approach: scored from 0 to 6 depending on depth and extent of cartilage loss. Intrachondral cartilage signal is scored as present or absent.	Subregional approach: each articular cartilage region is graded 0 to 3 for size of any cartilage loss as a % of surface area of each individual region surface, and % in this subregion that is full-thickness loss.	Subregional approach: focal and diffuse defects are differentiated. Depth of lesions is scored from 0 to 3. Diameter of lesions is scored from 0 to 3. Osteochondral defects are scored separately.
Bone marrow lesions	Scoring of individual lesions - 3 different aspects of BMLs are scored: A. Size of BML scored from 0 to 3 concerning % of subregional bone volume B. % of surface area adjacent to subchondral plate C. % of BML that is non-cystic	Summed BML size/volume for subregion from 0 to 3 based on % of subregional bone volume	Summed BML size/volume for subregion from 0 to 3 based on % of subregional bone volume. Number of BMLs counted. % of the volume of each BML that is non-cystic is graded from 0 to 3	Scoring of individual lesions from 0 to 3 based on maximum diameter of lesion
Subchondral cysts	Scored together with BMLs	Summed cyst size/volume for subregion from 0 to 3 in regard to % of subregional bone volume	Scored together with BMLs	Scoring of individual lesions from 0 to 3 based on maximum diameter of lesion
Osteophytes	Scored from 0 to 3 at 12 sites	Scored from 0 to 7 at 16 sites	Same as BLOKS: Scored from 0 to 3 at 12 sites	Scored from 0 to 3 Marginal intercondylar and central osteophytes are differentiated Locations/sites of osteophytes scoring not included
Bone attrition	Not scored	Scored from 0 to 3 in 14 subregions	Not scored	Not scored
Effusion	Scored from 0 to 3	Scored from 0 to 3	Scored from 0 to 3 (termed effusion-synovitis)	Scored from 0 to 3
Synovitis	A. scoring of size of	Combined	Scored from 0 to 3	Synovial thickening

	signal changes in Hoffa's fat pad B. Five additional sites scored as present or absent	effusion/synovitis score	(called Hoffa-synovitis)	scored as present or absent
Meniscal status	Intrasubstance signal changes in anterior horn, body, posterior horn scored separately in medial/lateral meniscus Presence/absence scored for the following: - intrameniscal signal, vertical tear, horizontal tear, complex tear, root tear, maceration, meniscal cyst	Anterior horn, body, posterior horn scored separately in medial/lateral meniscus from 0 to 4: 1. minor radial or parrot-beak tear 2. non displaced tear or prior surgical repair 3. displaced tear or partial resection 4. complete maceration or destruction or complete resection	Same as BLOKS, plus additional scoring for meniscal hypertrophy, partial maceration and progressive partial maceration.	No subregional division of meniscus described. Presence or absence of tears: - horizontal tear, vertical tear, radial tear, complex tear, bucket-handle tear, Meniscal intrasubstance degeneration scored from 0 to 3
Meniscal extrusion	Scored as medial and lateral extrusion on coronal image, and anterior extrusion for medial or lateral meniscus on sagittal image from 0 to 3	Not scored	Same as BLOKS	Scored on coronal image from 0 to 3
Ligaments	Cruciate ligaments scored as normal or complete tear Associated insertional BMLs are scored in tibia and in femur Collateral ligaments not scored	Cruciate ligaments and collateral ligaments scored as intact or torn	Same as BLOKS	Not scored
Periarticular features	Features are scored as present or absent: - patellar tendon signal, pes anserine bursitis, iliotibial band signal, popliteal cyst, infrapatellar bursa, prepatellar bursa, ganglion cysts of the tibiofibular joint, meniscus, ACL and PCL, semimembranosus, semitendinosus, other	Popliteal cysts, anserine bursitis, semimembranosus bursa, meniscal cyst, infrapatellar bursitis, prepatellar bursitis, tibiofibular cyst scored from 0 to 3	Same as BLOKS	Popliteal cysts only, scored from 0 to 3
Loose bodies	Scored as present or absent	Scored from 0 to 3 depending on number of loose bodies	Same as BLOKS	Not scored

Table 2. Comparison of technical aspects of each scoring system and their reliabilities

	BLOKS	WORMS	MOAKS	KOSS
MR imaging system used	1.5T system	1.5T system	3T system	1.5T system
MR imaging protocol of original publication	For reliability exercise (10 knees): sagittal/coronal T2-weighted fat-suppressed, sagittal T1-weighted spin-echo, axial/coronal 3D FLASH For validity of BML assessment (71 knees): sagittal proton density-weighted /T2-weighted, axial/coronal proton density-weighted /T2-weighted fat-suppressed	Axial T1-weighted spin-echo, coronal T1-weighted spin-echo, sagittal T1-weighted spin-echo, sagittal T2-weighted fat-suppressed, sagittal 3D SPGR	Coronal intermediate-weighted 2D turbo spin-echo, sagittal 3D DESS with axial/coronal reformation, sagittal intermediate-weighted fat-suppressed fast spin-echo	Coronal/sagittal T2-weighted and proton density-weighted, sagittal 3D SPGR, axial proton density-weighted and axial T2-weighted fat-suppressed
-Subregional division of knee	9 subregions: medial/lateral patella, medial/lateral trochlea, medial/lateral weight-bearing femur, medial/lateral weight-bearing tibia, subspinous tibia	15 subregions: medial/lateral patella, medial/lateral femur (anterior/central/posterior), medial/lateral tibia (anterior/central/posterior), subspinous tibia	15 subregions: medial/lateral patella, medial/lateral femur (trochlea/central/posterior), medial/lateral tibia (anterior/central/posterior), subspinous tibia	9 subregions: medial patella, patellar crest, lateral patella, medial/lateral trochlea, medial/lateral femoral condyle, medial/lateral tibial plateau
Inter-reader reliability	Based on 10 knees weighted-kappa between 0.51 (meniscal extrusion) and 0.79 (meniscal tear)	Based on 19 knees ICC between 0.74 (bone marrow abnormalities and synovitis/effusion) and 0.99 (cartilage)	Based on 20 knees weighted -kappa between 0.36 (tibial cartilage area) and 1.00 (patellar BML % cyst) % agreement between 55% (tibial osteophytes) and 100% (patellar BML % cyst)	Based on 25 knees weighted -kappa between 0.57 (osteochondral defects) and 0.88 (bone marrow edema)
Intra-reader reliability	Not presented	Not presented	Based on 20 knees weighted -kappa between 0.42 (Hoffa synovitis) and 1.00 (patellar BML size and	Based on 25 knees weighted -kappa between 0.56 (intrasubstance

			medial meniscal morphology) % agreement between 55% (Hoffa synovitis) and 100% (patellar BML size and medial meniscal morphology)	meniscal degeneration) and 0.91 (bone marrow edema and Baker cyst)

FLASH=fast low angle shot; DESS=dual echo steady state; SPGR=spoiled gradient echo.

Table 3. Summary of contrast-enhanced MR imaging-based semiquantitative scoring systems for synovitis in knee osteoarthritis

Publication	Rhodes et al	Modified Rhodes et al (used in Baker et al)	Guermazi et al
MRI system used	1.5T	1.5T	1.5T
Number of knees	35	454	400
MRI sequence	Axial T1-weighted fat-suppressed post contrast	Axial/sagittal T1-weighted fat-suppressed post contrast	Axial/sagittal T1-weighted fat-suppressed
Sites of synovitis evaluation	4 sites: Medial and lateral patellar recess, intercondylar notch and suprapatellar pouch (graded 0-3)	6 sites: Medial and lateral parapatellar recess, suprapatellar pouch and infrapatellar fat pad (graded 0-3) Medial & lateral posterior condyle (scored 0 or 1)	11 sites: Medial and lateral parapatellar recess, suprapatellar, infrapatellar, intercondylar, medial and lateral perimeniscal, and adjacent to anterior and posterior cruciate ligaments, adjacent to loose bodies, within Baker's cyst
Contrast administration	Gd-DTPA 0.2ml (0.1mmol)/kg body weight Post-contrast image acquired 4.5 minutes after injection	Gd-DTPA 0.2ml (0.1mmol)/kg body weight Post contrast axial image acquired 2 minutes after injection, immediately followed by sagittal image	Gd-DTPA 0.2ml (0.1mmol)/kg body weight Post contrast axial image acquired 2 minutes after injection, immediately followed by sagittal image
Grades	0=normal; 1=diffuse even thickening; 2=nodular thickening; 3=gross nodular thickening	0=normal; 1=diffuse even thickening; 2=nodular thickening; 3=gross nodular thickening	0=maximal synovial thickness < 2mm; 1=2-4mm; 2=greater than 4mm
Analysis approach	Synovitis assessed at each site only	Synovitis categories: 1. normal or questionable (<4 sites scored as 1 and all other sites scored as 0); 2. some (≥4 sites scored as 1 and/or ≤1 site scored as 2); 3. a lot (≥2 sites scored as 2 and no score of 3); 4. extensive (≥1 site scored as 3)	Whole-knee synovitis scores of 11 sites were summed and categorized: 0-4=normal or equivocal; 5-8=mild synovitis; 9-12=moderate synovitis; 13 or above=severe synovitis
Reliability	Not reported	Inter-reader: weighted-kappa 0.80 Intra-reader: weighted-kappa 0.58	For each site: Inter-reader, weighted -kappa 0.67-0.92; Intra-reader, weighted -kappa 0.67-1.00 (rater 1), 0.60-1.00 (rater 2) For summed score: Inter-reader, ICC 0.94; Intra-reader, 0.98 (reader 1), 0.96 (reader 2)

Gd=gadolinium; DTPA=diethylene triamine pentaacetic acid.